Re-Assessing the Need for Apatite- and Dolomite-Specific Calibrations of the Carbonate Clumped Isotope Thermometer

N. T. Anderson, M. Bonifacie, A. B. Jost, J. Siebert, T. Bontognali, J. Horita, I. A. Müller, S. M. Bernasconi, K. D. Bergmann

Geochemistry, Geophysics, Geosystems®

AGU ADVANCING EARTH AND SPACE SCIENCES

RESEARCH ARTICLE
10.1029/2023GC011049

Re-Assessing the Need for Apatite- and Dolomite-Specific Calibrations of the Carbonate Clumped Isotope Thermometer

N. T. Anderson[1], M. Bonifacie[2], A. B. Jost[1], J. Siebert[2], T. Bontognali[3,4], J. Horita[5], I. A. Müller[6], S. M. Bernasconi[7], and K. D. Bergmann[1]

[1]Massachusetts Institute of Technology, Cambridge, MA, USA, [2]Institut de Physique du Globe de Paris, Université de Paris Cité, Paris, France, [3]Space Exploration Institute, Neuchâtel, Switzerland, [4]University of Basel, Basel, Switzerland, [5]Texas Tech University, Lubbock, TX, USA, [6]University of Geneva, Geneva, Switzerland, [7]Geological Institute, ETH Zürich, Zürich, Switzerland

Abstract A few key methodological uncertainties remain for the carbonate clumped isotope community. One is how to compare data among published data sets that are not anchored to the InterCarb Carbon Dioxide Equilibrium Scale (I-CDES). A second is how temperature calibrations of calcite compare to those of other carbonate minerals in the I-CDES—particularly dolomite and apatite—which can elucidate several Earth system dynamics. Previous calibrations of the clumped isotope thermometer for dolomite are discrepant from one another and variably (dis)agree with calibrations developed for calcite; apatite calibrations have not yet been compared between laboratories using carbonate-based standardization. Here we report I-CDES standardized values for a suite of 11 carbonates that are commonly measured by the clumped isotope community to aid future comparisons of non-I-CDES data sets. In addition, 17 dolomite samples (25–1,200°C) and five apatite samples (1–38°C) of known precipitation temperature were measured using carbonate-based standardization. Excellent agreement between calcites and dolomites heated to similar temperatures (1,100–1,200°C) suggests no mineral-specific differences in absolute acid fractionation factor. We show that calcite and dolomite regressions largely agree but are sensitive to sample characteristics, regression method, and how equations are statistically compared. We suggest that there is no need for a dolomite-specific clumped isotope calibration, although our results suggest that further work is necessary to determine the influence of sample characteristics on this relationship. The apatite calibration equation defined in this study is statistically indistinguishable from calcite-based calibrations; we corroborate previous findings that an apatite-specific calibration is unnecessary.

Plain Language Summary The clumped isotope composition of carbonate rocks can teach geoscientists about the temperature and isotopic composition of ancient water masses. To be confident in measurements of clumped isotopes between laboratories, measurements should be compared to a common set of carbonate standards. Calculations of temperature based on clumped isotopes require empirical calibrations of carbonates with known formation temperatures. It is still uncertain if all carbonate minerals can use the same calibration. Here, we produce clumped isotope thermometer calibrations for the carbonate minerals dolomite and apatite. We show that these calibrations are statistically similar to calibrations for calcite in most cases and that dolomite- and apatite-specific clumped isotope calibrations are not necessary. We also extend the number and mineralogy of carbonate standards that have been assigned standardized values to facilitate easier data comparison between laboratories.

Key Points:

- Non-InterCarb carbonate standard values are presented and can be used to project data into the InterCarb Carbon Dioxide Equilibrium Scale
- We observe no dolomite-specific absolute acid fractionation factor
- We suggest that dolomite- and apatite-specific clumped isotope calibrations are unnecessary

Supporting Information:

Supporting Information may be found in the online version of this article.

Correspondence to:

N. T. Anderson,
nanderso@mit.edu

Citation:

Anderson, N. T., Bonifacie, M., Jost, A. B., Siebert, J., Bontognali, T., Horita, J., et al. (2024). Re-assessing the need for apatite- and dolomite-specific calibrations of the carbonate clumped isotope thermometer. *Geochemistry, Geophysics, Geosystems*, *25*, e2023GC011049. https://doi.org/10.1029/2023GC011049

Received 16 MAY 2023
Accepted 5 DEC 2023

Author Contributions:

Conceptualization: N. T. Anderson, M. Bonifacie, S. M. Bernasconi, K. D. Bergmann
Data curation: N. T. Anderson, M. Bonifacie, A. B. Jost, I. A. Müller, S. M. Bernasconi, K. D. Bergmann
Formal analysis: N. T. Anderson, A. B. Jost, S. M. Bernasconi, K. D. Bergmann
Funding acquisition: N. T. Anderson, K. D. Bergmann
Investigation: N. T. Anderson, M. Bonifacie, A. B. Jost, S. M. Bernasconi, K. D. Bergmann

1. Introduction

Carbonate clumped isotope thermometry has the potential to constrain the formation temperature ($T\Delta_{47}$) and oxygen isotope composition of formation water (water $\delta^{18}O$) of carbonate minerals by exploiting the thermodynamic preference for ^{13}C–^{18}O bonds in carbonate molecules with decreasing temperature (Eiler, 2007; Wang et al., 2004). $T\Delta_{47}$ and water $\delta^{18}O$ have important applications, including the temperature history of Earth's oceans (Barney & Grossman, 2022; Bergmann et al., 2018; Henkes et al., 2018; Meckler et al., 2022; Modestou et al., 2020), paleoaltimetry (Kelson et al., 2022), the diagenetic history of carbonates (Goldberg et al., 2021; Mackey et al., 2020; Shenton et al., 2015), and basin thermochronology and tectonics (Brigaud et al., 2020; Gasparrini et al., 2023; Mangenot et al., 2018). Most clumped isotope studies have focused on $CaCO_3$ polymorphs (calcite, aragonite) due to their ubiquity in the geologic record, pervasiveness in shells of biomineralizing

Methodology: N. T. Anderson, M. Bonifacie, A. B. Jost, J. Siebert, T. Bontognali, J. Horita, I. A. Müller, S. M. Bernasconi, K. D. Bergmann
Project Administration: N. T. Anderson, K. D. Bergmann
Resources: M. Bonifacie, J. Siebert, T. Bontognali, J. Horita, I. A. Müller, S. M. Bernasconi, K. D. Bergmann
Software: N. T. Anderson, A. B. Jost
Supervision: N. T. Anderson, K. D. Bergmann
Validation: N. T. Anderson, A. B. Jost, K. D. Bergmann
Visualization: N. T. Anderson, A. B. Jost
Writing – original draft: N. T. Anderson, K. D. Bergmann
Writing – review & editing: N. T. Anderson, M. Bonifacie, A. B. Jost, J. Siebert, T. Bontognali, J. Horita, I. A. Müller, S. M. Bernasconi, K. D. Bergmann

organisms, relative ease of laboratory precipitation, rapid dissolution in phosphoric acid, and generally better understood precipitation pathways.

However, the $T\Delta_{47}$ of other carbonate minerals can provide insights into key Earth history questions and have advantages over calcite or aragonite in select circumstances. Dolomite exists in the rock record as a precipitate of seawater, early diagenetic fluids, and burial diagenetic fluids; the Δ_{47} of dolomite can be used to constrain formation temperatures and the diagenetic history of carbonate rocks. While in many cases dolomite is a diagenetic phase, the comparatively lower solubility of dolomite and higher diagenetic activation energies for ^{13}C–^{18}O bond reordering (Hemingway & Henkes, 2020; Lloyd et al., 2018) can confer resistance to subsequent diagenesis. Clumped isotopes of structural carbonate bound in the lattice of apatite minerals are little studied but may provide a diagenetically-resistant phase to examine paleoenvironmental temperatures (Bergmann et al., 2018), habitat $\delta^{18}O$, and thermoregulation of toothed organisms and certain shelly fossils (Eagle et al., 2010; Löffler et al., 2019; Wacker et al., 2016). Tooth enamel is nearly anorganic, non-porous, highly crystalline and composed of large crystals with relatively few structural defects, rendering it highly resistant to isotopic alteration via post-depositional processes (Koch et al., 1997; LeGeros, 1981). Phosphatic inarticulate brachiopods have higher organic content than tooth enamel, but clumped isotopes of well-cleaned modern samples show good agreement with directly measured water temperature and select Cambro-Ordovician specimens show minimal evidence of diagenesis (Bergmann et al., 2018).

Two main challenges remain in attempts to use minerals other than calcite for clumped isotope studies. First, a wealth of clumped isotope data exists for both calcite and non-calcite data, but much of this is difficult to compare directly to more recent work because it was not run alongside carbonate standards that were assigned community consensus values during the InterCarb exercise (Bernasconi et al., 2021). Many carbonate clumped isotope labs use (or used) heated and equilibrated gases to project their Δ_{47} values into a common reference frame (the Carbon Dioxide Equilibrium Scale; CDES). A suite of internal (or "in-house") carbonate standards is often used to test the internal consistency of these measurements, to further correct measurements along with heated and equilibrated gases, or to compare results on identical samples with other labs. However, because the InterCarb exercise used a specific suite of carbonate standards that is (or was) not used in some labs, many studies lack carbonate standard values that allow projection into the I-CDES. To facilitate the projection of such data sets into the I-CDES and create a common framework for intercomparison, this study reports Δ_{47} values for 11 carbonate standards (including two dolomites) that are commonly used in clumped isotope studies. This data set overlaps and extends the non-InterCarb standards measured in Lucarelli et al. (2023) and Upadhyay et al. (2021); we report I-CDES Δ_{47} data for the standards TV-04, Rodolo, IPG-Sigal, IPG-TAR, CIT, and Depleted-Carb for the first time. With robust values for non-InterCarb standards, data from a wider range of clumped isotope studies can be compared in a common framework.

The second methodological challenge is that empirical calibrations for dolomite and particularly apatite have received less attention than that of calcite and have not been anchored to the InterCarb Carbon Dioxide Equilibrium Scale (I-CDES; Bernasconi et al., 2021) and, for dolomite, existing calibrations do not agree with each other (Bonifacie et al., 2017; Came et al., 2017; Müller et al., 2019; Winkelstern et al., 2016). Several empirical calibrations for the calcite clumped isotope thermometer have been created over the past ∼15 years (Anderson et al., 2021; Bernasconi et al., 2018; Ghosh et al., 2006; Huntington et al., 2009; Jautzy et al., 2021; Kele et al., 2015; Kelson et al., 2017; Petersen et al., 2019), and recent efforts using carbonate-based standardization (Bernasconi et al., 2021) and best practices in data reduction (Daëron, 2021) have converged on statistically indistinguishable calibration equations for calcite (Anderson et al., 2021; Fiebig et al., 2021; Jautzy et al., 2021). It is still disputed if mineral-specific calibrations are necessary or if a single clumped isotope calibration can be used for all (or a subset of) carbonate minerals (Bonifacie et al., 2017; de Winter et al., 2022; Guo et al., 2009; Hill et al., 2020; Holme et al., 2022; Löffler et al., 2019; Müller et al., 2019; Schauble et al., 2006; Winkelstern et al., 2016).

The four existing empirical dolomite clumped isotope thermometer calibrations (Bonifacie et al., 2017; Came et al., 2017; Müller et al., 2019; Winkelstern et al., 2016) came to diverging conclusions; Bonifacie et al. (2017) suggest that there is no statistically significant offset between calcite and dolomite calibrations, corroborating similar findings of Came et al. (2017) and Winkelstern et al. (2016). Anderson et al. (2021) tentatively suggested that dolomite and calcite could be described with a single calibration, but the small number of dolomite samples, lack of low- and high-temperature dolomite samples, and poor constraints of the reference frame for extremely

δ^{47}-depleted dolomites confounded the analysis. Two theoretical clumped isotope studies examining the effects of additional cations in the carbonate matrix support this result (Hill et al., 2020; Schauble et al., 2006). In contrast, Müller et al. (2019)—the sole study to use carbonate-based standardization—describe a calibration equation unique to dolomite. To calculate $T\Delta_{47}$ of dolomites confidently and consistently, community consensus on the calibration equation is necessary.

Four empirical calibrations of the apatite thermometer have been performed to date on a total of 22 unique samples; these studies suggest that structural carbonate associated with apatite follows the same calibration equation as calcite (Eagle et al., 2010; Griffiths et al., 2023; Löffler et al., 2019; Wacker et al., 2016) supporting the theoretical agreement between calcite and apatite demonstrated in Eagle et al. (2010). Griffiths et al. (2023) extended previous empirical work into the I-CDES and used an acid digestion temperature that is more typical in clumped isotope laboratories (90 vs. 110°C). We can test interlaboratory (in)consistency in measurements of apatite measured at different temperatures (90 vs. 70°C), test a different cleaning procedure (peroxide + acetic vs. no pre-treatment), and extend the temperature range of I-CDES-anchored apatite calibrations.

This study shares I-CDES values for a suite of non-InterCarb standards and provides new data that clarify the relationship between the calcite, dolomite, and apatite clumped isotope thermometer calibrations. We provide values for a suite of non-InterCarb carbonate standards (i.e., carbonate standards that were not assigned values by the clumped isotope community during the InterCarb exercise) projected into the I-CDES that can be used to compare clumped isotope data not run alongside InterCarb standards with data in the I-CDES. We also analyze a suite of dolomite calibration materials used in two previously discrepant dolomite calibration studies, four new dolomite samples heated to 1,100–1,200°C, and a new suite of apatite calibration materials using the same calcite-based standardization, well-replicated measurements, best practices in data reduction, and the same analytical process as a previous calibration shown to eliminate discrepancies in measurements of calcite samples (Anderson et al., 2021).

2. Materials and Methods

A total of 17 dolomites and five apatites spanning 1–1,200°C and a range of formation mechanisms were measured for this study, with samples originally from Bergmann et al. (2018), Bonifacie et al. (2017), Horita (2014), and Müller et al. (2019), as well as new samples collected and created for this study. Sample characteristics, including mineralogy, formation temperature, and magnesium concentration, are described in Table 1; sample-level data are in Table 2. Analysis-level data are reported in Table S1. More detailed data sets are available in the EarthChem database following the template of Petersen et al. (2019).

Eleven carbonates that have been used as internal carbonate standards in various laboratories were measured in this study, including two dolomites (Rodolo, SRM-88b) and nine calcites (CIT, Depleted Carb, 102-GC-AZ01, Carrara, IPG-TAR, NBS-19, IPG-Sigal, TV04). Sample characteristics and isotope values for this suite of samples are shown in Table 1, along with previously reported values for select standards included in Lucarelli et al. (2023) and Upadhyay et al. (2021).

2.1. Natural Dolomites

The dolomite sample Q1, interpreted as a primary precipitate (Brauchli et al., 2016), was extracted from a short core collected in the supratidal zone at 40 cm depth in the Dohat Faishakh sabkha on the western coast of the Qatar peninsula (see Müller et al., 2019). Long-term water temperature measurements do not exist for the sample location, but measurements from the same area (Illing et al., 1965) and estimates from well-studied analogous environments (Butler, 1969) constrain sample formation temperature to 32 ± 6°C. The 015 and 021 dolomite ordering peaks are clearly visible, but the 101 reflection is not (Müller et al., 2019).

The natural dolomite sample "BE" was collected from the Brejo do Espinho lagoon, about 100 km east of Rio de Janeiro. Lagoon water temperature at this location averages 25°C and annually varies by ±4°C. The sample was first treated with 0.1 M EDTA solution for ∼15 min to dissolve calcite and high-Mg calcite, with dolomite remaining, and then oxidized with 30% H_2O_2 overnight to remove organic matter (see Bonifacie et al., 2017).

2.2. Laboratory Dolomites

Laboratory (proto-)dolomites measured by Müller et al. (2019) were synthesized at the University of Leeds at 70, 140, and 220°C according to the method described by Rodriguez-Blanco et al. (2015). An amorphous gel-like

Table 1
Characteristics of Samples Measured in This Study

Sample	Orig. pub.	Mineralogy	Precip. method	Temp. (°C)	Temp. error (°C)	Ordering ratio (015/110)	Mol % Mg
Leeds 14	Müller et al. (2019)	Dolomite	Gel	140	2	0.21	48
Leeds 20	Müller et al. (2019)	Dolomite	Gel	70	2	0.08	42.7
Leeds 85	Müller et al. (2019)	Dolomite	Gel	220	2	0.39	50
Leeds 86	Müller et al. (2019)	Dolomite	Gel	220	2	0.4	51.5
150-A4	Bonifacie et al. (2017)	Dolomite	Powder	152.7	2	0.48	49.7
200-A1	Bonifacie et al. (2017)	Dolomite	Powder	201.6	2	0.35	48.9
300-A2	Bonifacie et al. (2017)	Dolomite	Powder	301.6	2	0.39	48.3
100-A3	Bonifacie et al. (2017)	Dolomite	Powder	102.3	2	0.1	42.3
250-A5	Bonifacie et al. (2017)	Dolomite	Powder	252.1	2	0.41	49.5
350-A9	Bonifacie et al. (2017)	Dolomite	Powder	351.4	2	Magnetite interference	50.4
80-1	Bonifacie et al. (2017)	Dolomite	Powder	80.2	2	N/A	46.7
DOLOMITE-1-HT	This study	Dolomite	Direct	1,200	10	–	–
BE	Bonifacie et al. (2017)	Dolomite	Natural	25	4	–	50.1
Q1	Müller et al. (2019)	Dolomite	Natural	32	6	0.29	49.5
Rodolo-HT	This study	Dolomite	Natural	1,100	10	–	–
Rodolo-quench	This study	Dolomite	Natural	1,100	10	–	–
Sansa-HT	This study	Dolomite	Natural	1,100	10	–	–
BISON_ENAMEL_A	This study	Apatite	Natural	38.7	1	–	–
CROCRO-A	This study	Apatite	Natural	25	5	–	–
GS-A	This study	Apatite	Natural	1	2	–	–
GS-B	This study	Apatite	Natural	1	2	–	–
JAPAN_IB	This study	Apatite	Natural	21	8	–	–
PM-B	This study	Apatite	Natural	38	3	–	–
CIT	Standard	Calcite	N/A	N/A	N/A	–	–
Depleted_Carb	Standard	Calcite	N/A	N/A	N/A	–	–
FAST-HAGA	Standard	Calcite	N/A	N/A	N/A	–	–
GCAZ-01b	Standard	Calcite	N/A	N/A	N/A	–	–
Hagit_Carrara	Standard	Calcite	N/A	N/A	N/A	–	–
IPG-Carrara	Standard	Calcite	N/A	N/A	N/A	–	–
IPG-Carrara-B2	Standard	Calcite	N/A	N/A	N/A	–	–
IPG-TAR	Standard	Calcite	N/A	N/A	N/A	–	–
NBS-19	Standard	Calcite	N/A	N/A	N/A	–	–
RODOLO	Standard	Dolomite	N/A	N/A	N/A	–	–
IPG-SIGAL	Standard	Calcite	N/A	N/A	N/A	–	–
SRM-88b-B2	Standard	Dolomite	N/A	N/A	N/A	–	–
TV-04	Standard	Calcite	N/A	N/A	N/A	–	–

solid was precipitated from a room temperature mixture of equimolar solutions of Na_2CO_3, $CaCl_2$, and $MgCl_2$ and followed by heating to the nominal temperature for between 1 day and 12 weeks (Müller et al., 2019). Experimental runs were quenched to room temperature in a cold-water bath after specified time intervals. Formation temperature uncertainty is ±2°C. X-ray Diffraction (XRD) patterns for the 70°C sample did not show the ordered 101, 015, and 021 dolomite reflections, suggesting a crystal structure of proto-dolomite; the 140°C sample showed 015 and 021 peaks but not 101, suggesting poorly ordered dolomite, and the 220°C sample showed all ordering peaks, consistent with ordered dolomite.

Table 2
Sample-Level Isotopic Data for Samples Measured in This Study

Sample	*N*	$\delta^{13}C$ (‰ VPDB)	$\delta^{18}O$ (‰ VPDB)	Δ_{47} (‰ I-CDES)	Δ_{47} 95% CI	δ^{47} (‰ VPDB)	$\Delta_{47\ Upadhyay}$ (‰ I-CDES)[a]	$\Delta_{47\ Lucarelli}$ (‰ I-CDES)[b]
Leeds 14	10	−7.4	−21	0.3850	0.0151	−28.4		
Leeds 20	11	−7.1	−14.8	0.4895	0.0149	−21.9		
Leeds 85	9	−7.5	−25	0.3096	0.0153	−32.5		
Leeds 86	10	−7.5	−24.9	0.3027	0.0151	−32.4		
150-A4	20	−50.5	−26	0.3544	0.0184	−76.5		
200-A1	8	−41.5	−26.9	0.3097	0.0211	−68.4		
300-A2	7	−42.7	−33.4	0.2486	0.0235	−76.1		
100-A3	13	−46.8	−17.5	0.4351	0.0153	−64.3		
250-A5	17	−53.4	−28	0.2673	0.0188	−81.4		
350-A9	13	−56.0	−32	0.2397	0.0184	−88.0		
80-1	15	−7.0	−16.4	0.4984	0.0115	−23.4		
DOLOMITE-1-HT	8	−0.5	−6.8	0.1802	0.0195	−7.3		
BE	10	−10.2	4.1	0.6070	0.0159	−6.1		
Q1	11	4.9	4.2	0.5864	0.0157	9.1		
Rodolo-HT	17	−4.0	1.8	0.1828	0.0209	−2.2		
Rodolo-quench	18	−4.0	1.7	0.1835	0.0143	−2.3		
Sansa-HT	14	1.4	−3.4	0.1844	0.0207	−2.0		
BISON_ENAMEL_A	12	−12.4	−12.4	0.5651	0.0152	−24.8		
CROCRO-A	15	−15.7	−1.4	0.5897	0.0127	−17.1		
GS-A	11	−2.71	−0.4	0.6602	0.0154	−3.11		
JAPAN_IB	7	−4.29	−2.2	0.6178	0.022	−6.5		
PM-B	11	−17.14	−7.8	0.5712	0.0154	−24.9		
CIT	11	2.05	−1.4	0.3236	0.0135	0.6	0.314	0.326
Depleted_Carb	22	−42.84	−20.3	0.4659	0.0150	−63.1		
102-GC-AZ01	17	0.86	−13.9	0.6086	0.0153	−13.0	0.62	0.598
Hagit_Carrara	13	2.25	−1.4	0.2966	0.0129	0.9	0.314	0.314
IAEA-C1	40	2.46	−2.1	0.3140	0.0069	0.4	0.3	0.299
IPG-INYO	27	−0.61	−7	0.2335	0.0088	−7.6		
IPG-Carrara	13	2.26	−1.4	0.2943	0.0124	0.9	0.314	0.314
IPG-Carrara-B2	10	2.26	−1.4	0.2930	0.0155	0.9	0.314	0.314
IPG-TAR	13	1.85	−15.8	0.2895	0.0124	−14.0		
MERCK	32	−42.42	−15.5	0.5169	0.0089	−57.9	0.522	0.514
NBS-19	9	1.96	−1.8	0.3154	0.0159	0.2	0.314	0.316
RODOLO	16	−3.79	3	0.6288	0.0116	−0.8		
IPG-SIGAL	19	−41	−7	0.4597	0.0141	−48.0		
SRM-88b-B2	18	2.1	−6.9	0.5209	0.0104	−4.8	0.499	0.528
TV-04	11	1.37	−8.3	0.5718	0.0148	−6.9		

[a]From Table 2 of Upadhyay et al. (2021). [b]From Table 4 of Lucarelli et al. (2023).

Synthetic dolomites for temperatures of 100, 150, 200, 250, 300, and 350°C described in Horita (2014) and measured by Bonifacie et al. (2017) were formed by reacting powdered $CaCO_3$ with Ca-Mg-(Na)-Cl solutions (Bonifacie et al., 2017; Horita, 2014). The reactor vessel was held at ±2°C of the nominal temperature for 6–85 days and then cooled quickly (<50°C in <30 min) by blowing with compressed air. These samples had

an attenuated 015 ordering reflection, consistent with some degree of dolomite ordering. The 80°C sample was formed via direct precipitation of proto-dolomite (i.e., lacking a 015 super-lattice peak) from a solution of $MgSO_4$, $Ca(NO_3)_2{\cdot}4H_2O$, and Na_2CO_3.

Four dolomite samples presented in this study were heated above 1,000°C. DOLOMITE-1-HT was generated at IPG Paris with a piston cylinder apparatus at 1,200°C (M. Bonifacie et al., 2023). Rodolo-HT, Rodolo-HT-quench, and Sansa-HT were created at ETH Zürich by heating the Rodolo and Sansa dolomite standards (both natural samples), respectively, at 1,100°C in a piston cylinder apparatus, following the procedure outlined in Müller et al. (2017).

2.3. Apatites

Tooth and shell materials from five species were analyzed in this study. All material was micro-drilled with a carbide bit and then powdered in an agate mortar and pestle to reduce grain size. Samples were not chemically pre-treated.

American crocodile (*Crocodylus acutus*) was obtained from the Harvard University Museum of Comparative Zoology collection and was originally from Bahía de Cabañas, Cuba. Reptilian body temperature estimates are not straightforward as they reflect both ambient environmental temperature and basking behavior (and other variables, such as body size); we use a temperature of 28.7 ± 5°C derived from an average of fasted versus fed *C. acutus* body temperatures from the study of Lang (1979). *Lingula* brachiopod valves were collected from the tidal flats of Ariake Bay, Japan (see Bergmann et al., 2018); a formation temperature of 21 ± 8°C was assigned on the basis of annual NOAA satellite-derived seawater temperature estimates at Yatsushiro, Japan. Greenland shark teeth were purchased and have an assumed formation temperature of 2 ± 1°C (Watanabe et al., 2015). American bison (*Bison bison*) and American marten (*Martes americana*) teeth were also purchased and have typical body temperatures of 38.7°C (Hawley & Peden, 1982) and 38°C (Clarke et al., 2010) respectively.

2.4. Mass Spectrometry and Data Reduction

Mass spectrometry methods were nearly identical to those reported in Anderson et al. (2021; excepting samples Rodolo-HT, Rodolo-HT-quench, and Sansa-HT). Sample $\Delta_{47,}$ $\delta^{18}O$, and $\delta^{13}C$ were measured from January 2018 to November 2022 at the MIT Carbonate Research Laboratory on a Nu Perspective dual-inlet isotope ratio mass spectrometer with a Nu Carb automated sample preparation unit held at 70°C (see Mackey et al., 2020). Dolomite samples weighing ∼400–600 μg and apatite samples weighing ∼5–20 mg were reacted for 25 or 90 min in individual glass vials with 150 μL orthophosphoric acid (ρ = 1.94 g/cm^3). Evolved CO_2 gas was purified cryogenically and by passive passage through a Porapak trap (1/4″ ID; 0.4 g 50/80 mesh Porapak Q) held at −30°C. Purified sample gas and reference gas of known composition were alternately measured on six Faraday collectors (m/z 44–49) in 3 acquisitions of 20 cycles, each with 20 s integration time (i.e., 60 cycles with 20 min total integration time). The initial voltage was 8–20 V on the m/z 44 beam with 2×10^8 Ω resistors and was depleted by approximately 50% over the course of an analysis. Sample and standard CO_2 gases were depleted at equivalent rates from microvolumes over the analysis time.

Each session of approximately 50 individual analyses began with each of ETH-1–4 in random order, and then alternated between blocks of three unknowns and two ETH anchors. Additionally, IAEA-C1, IAEA-C2, Merck, and Rodolo (La Roda dolomite; see García del Cura et al., 2001 and Müller et al., 2017) were each measured once per run; NIST SRM-88b (a dolomite standard) was analyzed twice per run as a dolomite-specific check of the accuracy of the data set and for potential future reassessment of dolomite analyses once inter-laboratory accepted dolomite anchor values are available. ETH-1–4 and IAEA-C2 were used as anchors; other standards were treated as unknowns. Unknown:anchor ratio was planned at 1:1 for each run. The reference side of the dual-inlet was refilled with reference gas after every 10 analyses. In total, unknowns were measured 7–17 times over the study interval (483 total unknown analyses; 243 "non-InterCarb" standards, 180 dolomite, 60 apatite).

Raw mass spectrometer data were first processed by removing cycles (i.e., single integration cycles of mass spectrometer measurement) with raw Δ_{47} values more than 5 "long-term" standard deviations (0.50‰; the mean of the respective cycle-level SD for ETH-1–4 over a 3-month period was 0.10‰) away from the median Δ_{47} measurement for the analysis (0.2% of cycles removed). Analyses were removed if more than 10 cycles (out of 60 total cycles) fell outside the 5 long-term SD threshold. Analyses with transducer pressure below 15 mbar, typically

corresponding to sample collection issues or incomplete digestion, and analyses that ran misbalanced between sample and reference sides by >1% were also removed. No pressure baseline correction was applied. Long-term external repeatability (1SD) of Δ_{47} for all analyses (anchors and unknowns) after the data processing described above, including the error introduced by the reference frame, is 0.021‰.

After the removal of cycle-level outliers, data were processed using the "D47crunch" Python package using IUPAC ^{17}O parameters, 70°C ^{18}O acid fractionation factor of 1.00871 for apatite (Kim et al., 2007) and 1.009926 for dolomite (Rosenbaum and Shepard, 1986), and projected to the I-CDES with values for ETH-1–4 and IAEA-C2 anchors from the InterCarb project (Bernasconi et al., 2021; Daëron, 2021). Raw Δ_{47} measurements were converted to the I-CDES using a pooled-regression approach that accounts for the relative mapping of all samples in δ^{47}-Δ_{47} space (Daëron, 2021). Analytical uncertainty and error associated with the creation of the reference frame were fully propagated through the data set. A full description of the data reduction procedure used in D47crunch is detailed in Daëron (2021). Each sample carousel (typically 50 analyses) was treated as a single analytical session. IAEA-C1 and Merck standards were treated as unknowns and used as an internal consistency check (IAEA-C1 mean Δ_{47} = 0.314‰ vs. nominal Δ_{47} = 0.302‰, 1SD = 0.017‰; Merck mean Δ_{47} = 0.517‰ vs. nominal Δ_{47} = 0.514‰, 1SD = 0.019‰). As a test of reproducibility of well-replicated standards (>4x per run) and to assess potential drift associated with the reference frame, ETH-4 was temporarily treated as an unknown (ETH-4 mean Δ_{47} = 0.446‰ vs. nominal Δ_{47} = 0.451‰, 1SD = 0.019‰); there was no relationship between Δ_{47} residual and analysis time (R^2 = 0.003, Figure S1 in Supporting Information S1). Finally, Peirce's criterion (Ross, 2003; Zaarur et al., 2013) was applied iteratively to the data set at the analysis level to remove outliers. Four unknown analyses were marked as outliers and removed, followed by reprocessing the data set.

Oxygen, carbon, and clumped isotope compositions of Rodolo-HT, Rodolo-HT-quench, and Sansa-HT were measured at ETH-Zurich on a MAT 253 IRMS coupled to a Kiel IV carbonate sample preparation device. Samples and standards weighing 130–160 µg reacted at 70°C with 104% phosphoric acid. The sample gas was measured once for 600 s, followed by an equal length measurement of reference gas. Measurements began at 20–25 V on mass 44 and decreased by ∼10 V over the course of the analysis. Further details on mass spectrometry for these samples can be found in Müller et al. (2019).

Raw data from Müller et al. (2019), originally processed using Easotope with carbonate anchor values from Bernasconi et al. (2018), were reprocessed in this study using Easotope with updated carbonate anchor values from the InterCarb exercise (Bernasconi et al., 2021); new data for Rodolo-HT, Rodolo-HT-quench, and Sansa-HT were corrected using the same method. Easotope uses a "moving-window" standardization approach, whereas D47crunch uses a pooled regression model of all analyses (anchors and unknowns); the moving-window approach is more appropriate for the Müller et al. (2019) data set given the distribution of InterCarb anchors. The average Δ_{47} offset between previously published and reprocessed data is 16 ppm (Table S2).

Data from Table S2, Bonifacie et al. (2017; IPG only) were reprojected into the I-CDES using the "D47crunch" package (Daëron, 2021) with seven carbonate anchors (IPG-Carrara, 102-GC-AZ01, NBS-19, IAEA-C1, IPG-SIGAL, ETH-1, and ETH-2); 28 of 34 anchor measurements were IPG-Carrara or 102-GC-AZ01. Values for carbonate standards presented in this study (Table 2) were used for the reprojection.

Linear regressions of Δ_{47} and $10^6/T^2$ data were performed in two ways: first, a Monte Carlo approach, in which the entire data set was resampled 10,000 times at the analysis level; then a formation temperature was randomly selected from a normal distribution defined by uncertainty in formation temperature for each bootstrap; finally, a linear regression was fit through each of these resampled data sets. This is similar to the method used by Petersen et al. (2019). In the second approach, "York" regression was calculated accounting for propagated error in Δ_{47} (95% CL) and stated error in temperature (York et al., 2004; Zaarur et al., 2013). These two regression methods were found to give slopes within 0.00002 and intercepts within 0.0006 of each other, approximately an order of magnitude less than the error of the regressions. The equations reported below use the Monte Carlo approach. Analysis of covariance (ANCOVA) was performed using 1SD external reproducibility and a confidence level of p = 0.05 for significance.

3. Results and Discussion

3.1. Non-InterCarb Standards

This study reports Δ_{47} values for 11 carbonate standards (including two dolomites) that are commonly used in clumped isotope studies. This data set overlaps and extends the non-InterCarb standards measured in other

studies (Lucarelli et al., 2023; Upadhyay et al., 2021); we report I-CDES Δ_{47} data for the standards TV-04, Rodolo, IPG-Sigal, IPG-TAR, CIT, and Depleted-Carb for the first time. We show excellent agreement with the data of Lucarelli et al. (2023) and Upadhyay et al. (2021) on samples that were measured by both labs, with an average Δ_{47} difference of 8 and 6 ppm, respectively—below analytical uncertainty—despite differences in sample preparation, measurement, and data processing. This excellent overall agreement provides a vote of confidence for the InterCarb exercise. SRM-88b, the sole dolomite standard measured among the three labs with respect to the I-CDES (Table 2), showed perfect agreement between this study ($\Delta_{47} = 0.528$) and Lucarelli et al. (2023; $\Delta_{47} = 0.528$), but an offset outside of analytical uncertainty with Upadhyay et al. (2021; $\Delta_{47} = 0.499$).

Clumped isotope composition for these non-InterCarb standards projected to the I-CDES using anchor values from the InterCarb exercise are reported in Table 1. An example Python script to standardize non-InterCarb data, based on the "Δ_{47}crunch" module (Daëron, 2021), is shown in Supporting Information S1. Using this approach, data sets with sufficient measurements of these non-InterCarb standards can be projected into the I-CDES. The full suite of non-InterCarb standards measured here encompasses a wide range of δ^{47}-Δ_{47} space (Figure S2 in Supporting Information S1), although individual studies typically only use ∼1–3 unique carbonate standards. Dolomite non-InterCarb anchors measured here (SRM-88b and Rodolo) and in other studies (Defliese et al., 2015; Lucarelli et al., 2023; Müller et al., 2019; Murray et al., 2016; Upadhyay et al., 2021) have a relatively narrow range of Δ_{47} (0.52–0.63‰) and δ^{47} (−0.8–4.8‰; Figure S2 in Supporting Information S1). Furthermore, as shown above, various studies have provided different values for dolomite standards. To facilitate better intercomparison of dolomite clumped isotope values from different laboratories, we suggest that the community adopts a suite of dolomite standards with a wide range of clumped and bulk isotope compositions that approximate those of the InterCarb standards. As in the InterCarb exercise, these standards should be measured at several laboratories and a consensus value should be adopted by the clumped isotope community.

This method can be applied to any historical data set that contains two or more carbonate standards listed in Table 1, but will tend to have lower uncertainty as the carbonate standard:sample ratio increases, as particular standards were run more consistently throughout sessions, and as the δ^{47}-Δ_{47} space bracketed by samples better overlaps the δ^{47}-Δ_{47} of unknowns.

We attempted to apply this method to the dolomite calibration data of Bonifacie et al. (2017) and Winkelstern et al. (2016) to allow data inter-comparison within the I-CDES. Only one carbonate standard of those assigned I-CDES values in this study or in Upadhyay et al. (2021; Carrara Marble) was measured in Winkelstern et al. (2016), disqualifying the study from re-projection into the I-CDES.

Bonifacie et al. (2017) included a total of seven such samples, although only 102-GC-AZ01 and IPG-Carrara had more than two analyses. This allows us to carry out the re-projection, with the following caveats: (a) 34:109 anchors with known I-CDES values to unknown ratio (compared to 1:1 in this study) is exacerbated by the uneven distribution of carbonate standards; (b) no dolomite standards; (c) the carbonate standards were not designed to bracket extremely depleted samples (see Section 3.2.4 for further discussion) because this was done with heated and equilibrated gases in the original study; (d) sufficient data for re-analysis are only available from a portion of the data. Finally, only measurements performed at IPG Paris for the Bonifacie et al. (2017) have sufficient data and metadata to facilitate re-projection. While these limitations cast doubt on the usefulness of comparisons of re-projections of this data set to data intentionally generated in the I-CDES, we see good agreement between the re-projected IPG-only Bonifacie et al. (2017) data set and this study (average 15 ppm offset; see Table S3, Figure S3 in Supporting Information S1), although it is larger than the offset between the CDES IPG-only Bonifacie et al. (2017) data and this study (10 ppm; see Table S3). One subset of samples show excellent agreement (200-A1, 300-A2, 100-A3, 250-A5; 4 ppm offset), while 150-A4, 350-A9, 80-1, and BE show significant offset (26 ppm; higher than repeatability for this study). The mean 95% confidence level (CL) for I-CDES Bonifacie et al. (2017) data is approximately double that of the originally published data (31 vs. 16 ppm; Table S3). Ultimately, the reprojection of Bonifacie et al. (2017) data using non-InterCarb carbonate standards gives reasonable results, but because of the reasons mentioned above, we choose to use the original Bonifacie et al. (2017) CDES data when comparing dolomite calibration equations.

While we do not prescribe any "thresholds" for which data sets are appropriate for reprojecting to the I-CDES, we note that anchor:unknown ratio, anchor distribution throughout analytical sessions, anchor mineralogy, overlap of anchor and unknown bulk/clumped isotope composition, and precision to which anchor values are known

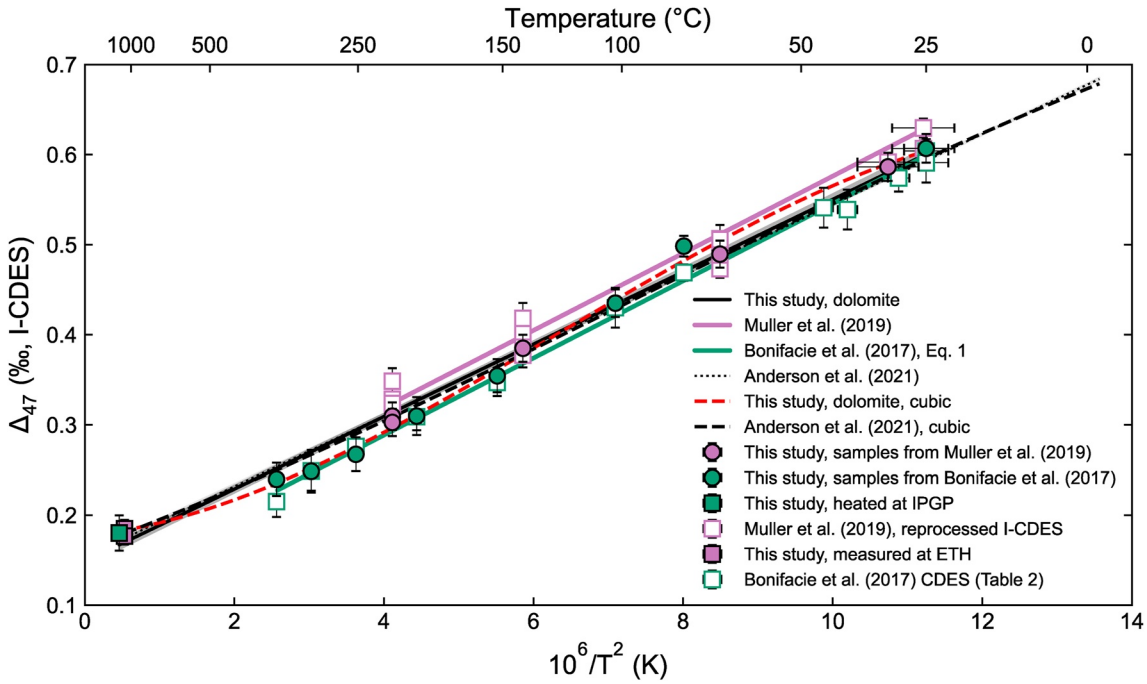

Figure 1. Linear (black) and third-order (red dashed) $1/T^2$-Δ_{47} regressions for dolomite samples measured in this study and that from Anderson et al. (2021). Filled circles represent samples measured in this study that were originally analyzed by Bonifacie et al. (2017; green) and Müller et al. (2019; purple). Filled squares show new samples produced and measured in this study. Open squares show data from the same samples in their original studies, with Bonifacie et al. (2017) data reported with respect to the CDES90 reference frame and Müller et al. (2019) re-processed to the InterCarb Carbon Dioxide Equilibrium Scale (I-CDES) reference frame. Linear regressions through these data agree with Anderson et al. (2021) using analysis of covariance (ANCOVA) and 1 SD error of the estimate; third-order regressions do not agree within 1 SD error of the estimate (see Table 3 and Table S4).

(both in number of replicates measured, and in number of labs that have measured the standard) are all important considerations that make when attempting to project data into the I-CDES.

3.2. Calibration of the Dolomite Clumped Isotope Thermometer

3.2.1. Comparison to Previous Dolomite and Calcite Calibrations

To determine the statistical agreement of this study with previous empirical calibrations, we use (a) ANCOVA and (b) standard deviation of bootstrapped regressions to compare it to the calibration of Anderson et al. (2021) because the core data set from each calibration was created under nearly identical conditions in the same laboratory. We use Equation 1 from Anderson et al. (2021), which includes data from other recent I-CDES calibrations (Jautzy et al., 2021; Meinicke et al., 2020; Peral et al., 2018), all shown to be statistically indistinguishable from one another and from the calibration of Anderson et al. (2021).

When all samples are considered, the linear dolomite Δ_{47}-$1/T^2$ regression of data presented here (Figure 1, Table 3) is statistically indistinguishable from the calibration equation of Anderson et al. (2021) using ANCOVA at the $p > 0.05$ level with a 2 SD external Δ_{47} uncertainty (44 ppm) and is within 1 SD error of the regression for intercept, but narrowly misses this threshold for slope (Table 3). The linear dolomite regression from this study has a slightly lower intercept and steeper slope than Anderson et al. (2021), with a calculated temperature of ~2°C greater than calcite at earth-surface temperatures fading to parity at ~250°C and with calculated dolomite temperatures lower than calcite for dolomites formed >250°C (Figure 2).

A third-order polynomial regression through the data from this study, on the other hand, diverges from the third-order fit of Anderson et al. (2021); two of the four polynomial fit coefficients fall outside the 1 SD threshold (Figure 1, Table S4). In the following sections, we explore potential justifications for the offset between the third-order calibration produced in this study and in Anderson et al. (2021), including the incomplete reaction of carbonate, a mineral-specific acid fractionation factor, lack of constraint by carbonate anchors, magnesium concentration, cation ordering, or precipitation kinetics.

Table 3
Results of Bootstrapped Regressions and Analysis of Covariance (ANCOVA) for Subsets of Data in This Study

Data set	Slope[a]	Intercept[a]	Slope SD	Int. SD	p_{slope}[b]	p_{int}[b]
Anderson et al. (2021)	0.0391	0.154	0.0003	0.0030	1	1
This study, all dolomite	0.0401	0.1487	0.0006	0.0040	0.38	0.64
This study, all apatite	0.0302	0.2577	0.0025	0.0281	0.31	0.49
This study, dolomite $\delta_{47} > -30$	0.0398	0.1593	0.0006	0.0046	0.60	0.02
This study and Müller et al. (2019)	0.0406	0.1520	0.0005	0.0033	0.12	0.09
This study and Müller et al. (2019) $\delta_{47} > -30$	0.0400	0.1599	0.0005	0.0036	0.49	0.00
This study, gel or natural precipitates	0.0392	0.1593	0.0006	0.0047	0.93	0.12
This study and Müller et al. (2019), gel or natural precipitates	0.0398	0.1598	0.0005	0.0035	0.70	0.00
This study, apatites, versus Griffiths et al. (2023)[c]	0.0325	0.2240	0.0093	0.1160	0.99	0.90

[a]Calculated using bootstrap approach (see Methods) with a normal distribution of formation temperature. [b]ANCOVA *p*-values for comparison to Anderson et al. (2021); 2SD repeatability used for error. [c]ANCOVA *p*-values for comparison between apatites in this study, and Griffiths et al. (2023).

3.2.2. Effects of Reaction Time

The reaction duration between phosphoric acid and carbonate powder may affect Δ_{47} values through two mechanisms: (a) incomplete dissolution of a carbonate phase and (b) undesired reactions between phosphoric acid, water, and liberated CO_2 during the dissolution process. Longer reactions also increase the possibility of substantial atmospheric CO_2/H_2O contamination. We tested the potential effects of reaction time by measuring a subset of dolomite samples with 25 and 90 min acid reaction times (all at 70°C).

We show that complete acidification of dolomites (within 95% CL of the 205 analyses of ETH-1, a pure calcite) occurs in 25 min for most samples (Figure S4 in Supporting Information S1; note that 350-A9 is ~75% carbonate and ~25% magnetite), with 80-1, Q1, and Leeds 14 showing average CO_2 evolution around 80%. Because Q1 is

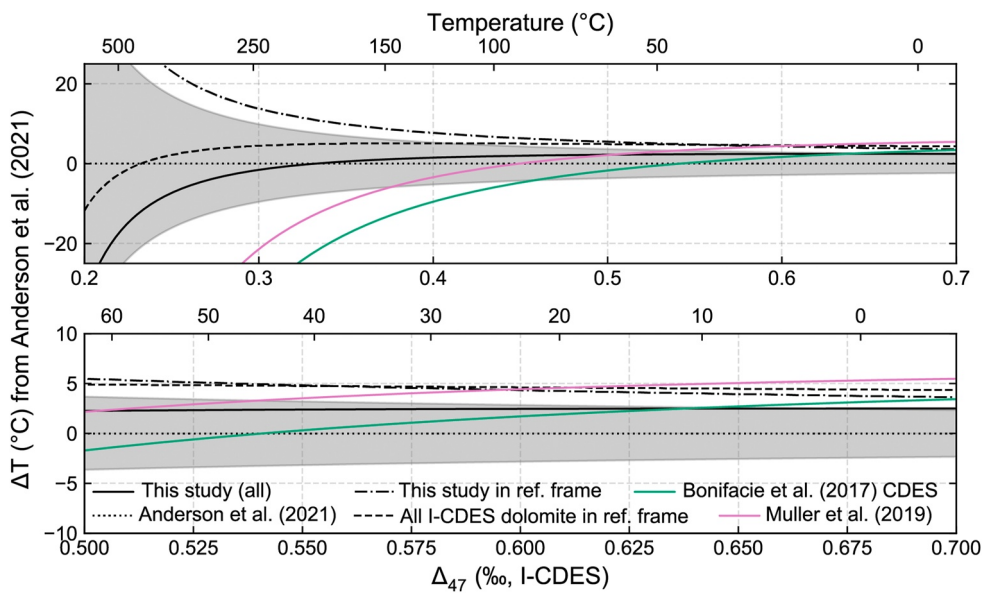

Figure 2. Comparison of calculated temperatures for 0–500°C (top panel) and 0–60°C (bottom panel) using regressions through all data in this study, all data in this study with δ^{47} values >−30, and all data in this study with δ^{47} values >−30 plus the data from Müller et al. (2019) reprocessed into the InterCarb Carbon Dioxide Equilibrium Scale (I-CDES). The regression from Equation 1 of Anderson et al. (2021) is used to calculate the datum; the Δ_{47}-T relationships of Bonifacie et al. (2017), Müller et al. (2019), and Petersen et al. (2019) are shown for comparison. The calculated temperatures based on regression through all data in this study are 0–3°C higher than the calculated temperatures from Anderson et al. (2021) until ~250°C, where they become lower.

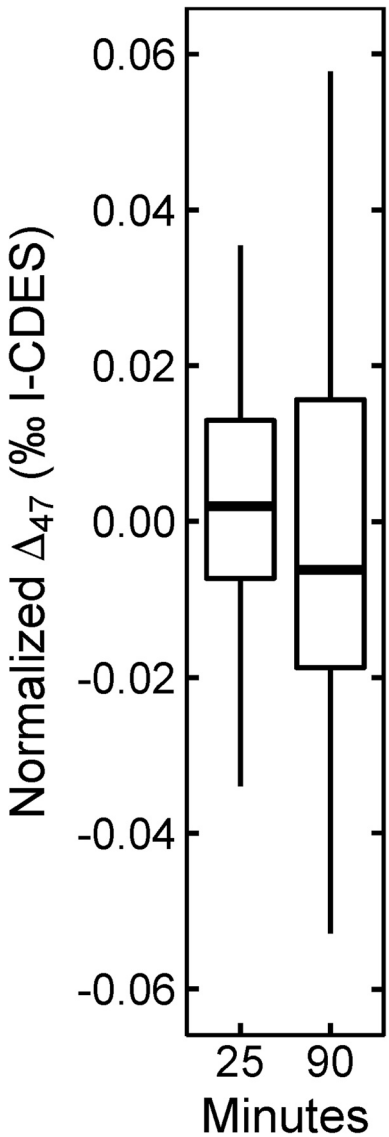

Figure 3. Comparison of normalized Δ_{47} values for a subset of samples that were run at both 25 and 90 min acid reaction time. There is no statistically significant difference in Δ_{47} between these two populations.

a natural evaporative precipitate and thus may contain non-carbonate material (potentially poorly crystalline silicates) and does not have evidence of improved dissolution in 90 min, we infer quantitative dissolution of carbonate. 80-1 also shows no improvement with 90 min reaction times, although it is a laboratory precipitate. Two samples, originally from Müller et al. (2019), show up to ~20% greater dissolution in 90 min reaction time (Figure S4 in Supporting Information S1), suggesting incomplete dissolution of carbonate in 25 min. We note that a 90-min reaction time causes a ~50% increase in Δ_{47} uncertainty in our analytical system; 1SD uncertainty is 22 ppm for 90-min reactions and 14 ppm for 25-min reactions. We speculate that this could be from subtle ingress of atmospheric CO_2/H_2O as the reaction progresses or from increased interaction time of the CO_2-H_2O-H_3PO_4 system.

Despite some evidence for incomplete digestion in isolated samples and greater uncertainty with longer reactions, we see no statistically significant effect of acid digestion duration on Δ_{47} or $T\Delta_{47}$ at the population level (Figure 3). This observation corroborates the findings of Müller et al. (2019), who similarly saw no Δ_{47} effect of reaction time. One individual sample, the dolomite standard Rodolo, does show a significant difference in Δ_{47} for 25 versus 90 min reaction time ($p < 0.05$ via t-test; although $p > 0.05$ via Wilcoxon rank-sum test; Figure S5 in Supporting Information S1). Because Rodolo is not used as an anchor and is not a calibration sample, all samples used as anchors or as unknowns in the calibration regression show no statistically significant effect from reaction duration. This agreement between analyses at 25 and 90 min reaction times corroborates the results of Bonifacie et al. (2017) for 90°C reactions, in which no measurable difference was found between analyses performed at Caltech (20 min reaction time) and IPG Paris (120 min reaction time). Therefore, we combine analyses performed at both reaction durations to compute the regressions throughout this study. We recommend that sample powders be ground finely using a mortar and pestle to increase the reaction rate and urge future researchers to report the CO_2 yield of both unknowns and anchors relative to a pure calcite standard.

3.2.3. Is There a Mineral-Specific Absolute Acid Fractionation Factor?

A common hypothesis to explain potential differences between clumped isotope measurements of dolomite and calcite is that the "absolute" acid fractionation factor (cf. "PAFF" in Lu et al., 2022 and Δ_* in Bonifacie et al., 2017) is offset between the two minerals (irrespective of any AFF derived from different acid reaction temperatures). Various authors have attempted to quantify this offset (Defliese et al., 2015; Lu et al., 2022; Müller et al., 2017; Murray et al., 2016). The dependence of the absolute AFF on acid dissolution temperature hampers these interpretations; it is possible that a dolomite-specific absolute AFF is necessary only at particular acid digestion temperatures (Lu et al., 2022; Müller et al., 2019). Furthermore, a recent study has suggested that dolomite absolute AFF may be dependent on the Δ_{47} value of the dolomite sample (Lu et al., 2022). The uncertainty related to the absolute AFF can cause large differences in the calculated temperature.

The "variable AFF" presented by Lu et al. (2022) suggests that dolomite absolute AFF is dependent on the Δ_{47} value of the sample, with more rapid exchange of CO_2 with the H_2O-H_3PO_4 system occurring when the difference between the Δ_{47} of the sample and the theoretical equilibrium value at a given acid temperature is larger, particularly during longer reactions (Lu et al., 2022; Swart et al., 2019). Applying the Lu et al. (2022) variable AFF to this dolomite data set lowers the intercept and steepens the slope of the linear regression, worsening the agreement with previous calibrations. For the third order regression, three out of four regression coefficients show worse agreement with Anderson et al. (2021) when the variable AFF is applied. This observation does not argue against the existence of a dolomite-specific absolute AFF but shows that it cannot be invoked to explain the offset between third-order calcite and dolomite calibrations described in Section 3.2.1.

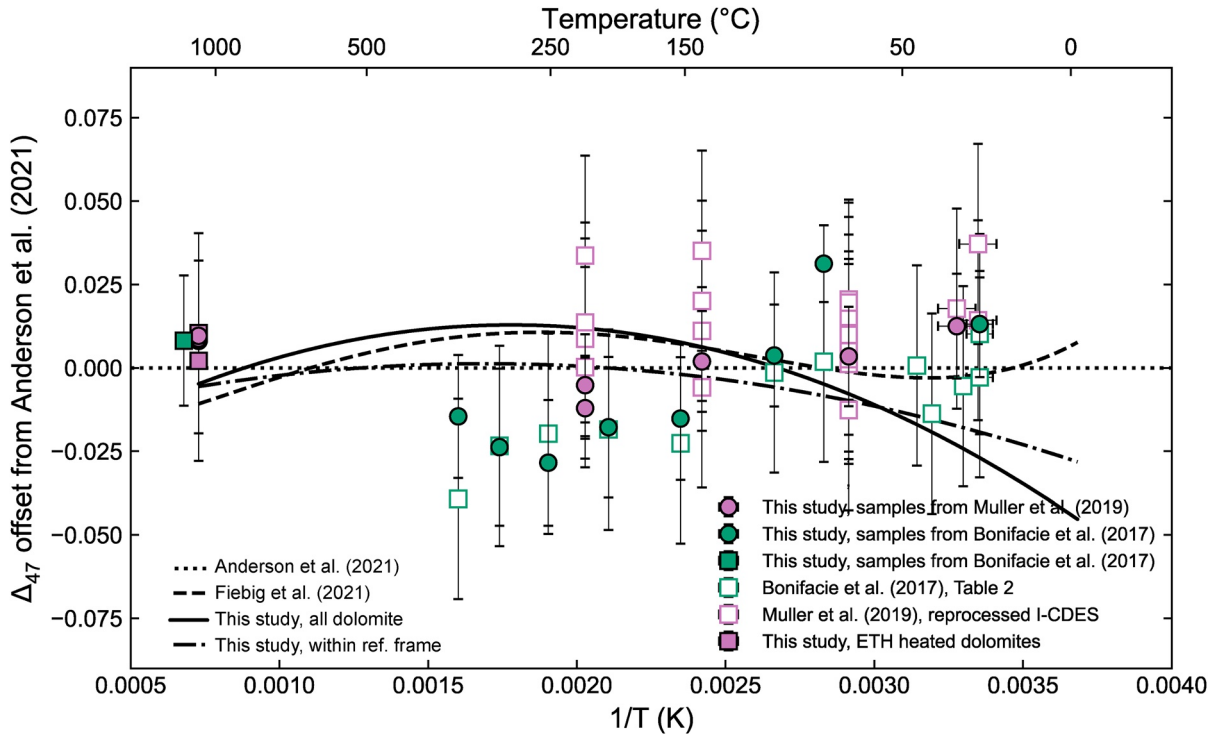

Figure 4. Solid symbols show difference in Δ_{47} between dolomite samples measured in this study (closed shapes), measured values from previous studies (open shapes), and the prediction from the Anderson et al. (2021) calibration. Lines compare regressions from subsets of data from this study with Anderson et al. (2021) and Fiebig et al. (2021).

We can directly test the agreement of the calcite and dolomite absolute AFF using minerals heated to near-stochastic temperatures; a significant offset at very high temperatures would suggest (and quantify) a mineral-specific absolute AFF. Four heated dolomite samples reported in this study (three formed at ETH at 1,100°C and measured at ETH; one formed at IPG Paris at 1,200°C and measured at MIT) have Δ_{47} values within 10 ppm of those predicted for calcites with the Anderson et al. (2021) calibration equation (Figure 4). These heated dolomites (DOLOMITE-1-HT, Rodolo_HT, Rodolo_quench, and Sansa_HT) give Δ_{47} values of 0.180, 0.183, 0.184, and 0.184‰, respectively (Table 2); calcites heated to 1,100°C and measured at MIT as part of a previous study give Δ_{47} values of 0.178 and 0.192‰ (Anderson et al., 2021), well within error of dolomites formed at the same temperature. These data for near-stochastic samples demonstrate no resolvable difference in absolute acid fractionation factors between dolomite and calcite in the samples analyzed here.

3.2.4. Considerations for Samples Not Contained by Carbonate Anchors

While the δ^{47}-Δ_{47} space defined by InterCarb calcite anchors contains most samples found in nature, a subset of the laboratory precipitates in this study are extremely depleted in δ^{47} (approx. −70 to −90‰; Figure 5a), far outside of the I-CDES reference frame. Merck, the most δ^{47}-depleted InterCarb anchor at approximately −60‰, was measured along with the dolomite calibration data set, but we do not include it as an anchor for three reasons. First, while Merck is the most depleted I-CDES anchor, it is still approximately 10–30‰ more enriched than the most depleted unknowns in this study; even when Merck is used as an anchor, considerable extrapolation of the reference frame is necessary. Second, to maintain consistency with the calcite calibration measured using identical analytical conditions (Anderson et al., 2021), Merck was only analyzed once per run of 50 replicates, leading to relatively high uncertainty compared to other carbonate anchors. Finally, the value of Merck itself is poorly constrained with respect to the other InterCarb anchors (Bernasconi et al., 2021), with an uncertainty roughly double IAEA-C1's uncertainty, and with some labs reporting mean values ∼50 ppm from the community consensus value from the InterCarb exercise (cf. max ∼25 ppm offset for IAEA-C1). When we process Merck as an unknown, we calculate its Δ_{47} value to be 0.517, just ∼3 ppm from the consensus value. It is encouraging that measurements of an "unknown" outside the I-CDES reference frame can agree so closely with the established value, but it is unclear whether this extends to even lower δ^{47} values. There is also close agreement of the Δ_{47}

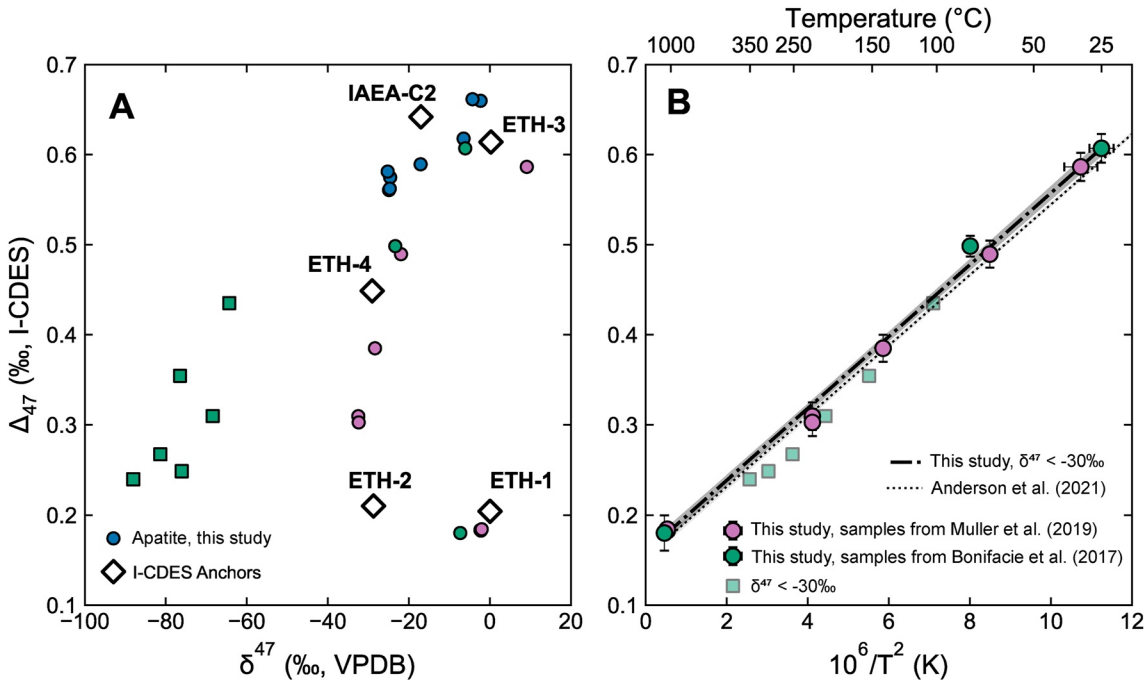

Figure 5. (a) Δ_{47} and bulk isotopic composition (δ^{47}) of samples measured in this study. Most samples are contained in the Δ_{47}-δ^{47} space defined by the ETH anchors, but green squares show samples that are outside this space. (b) Regression of dolomite samples with δ^{47} values constrained by ETH anchors closely match that of Anderson et al. (2021).

values from the extremely depleted samples used in both this study and in Bonifacie et al. (2017; see Figure 5b), which used low δ^{47} heated and equilibrated gases–only 15‰ away from the lowest δ^{47} values for unknowns–for data correction.

Yet moving outside the reference frame increases the uncertainty in projecting raw Δ_{47} values to the I-CDES reference frame (95% CL = 0.019‰ for extremely depleted samples; 0.013‰ for all other samples, despite higher *n* for depleted samples). Given that the extremely depleted samples measured here solely define the calibration for the 250–350°C temperature range and exert a large influence on the calibration (78 of 139 dolomite calibration replicates under 1,100°C), particularly for the third-order regression, we tested the response of the calibration to the removal of these samples (Figure 5b). ANCOVA shows that the calibration regression for all dolomite samples within the I-CDES reference frame is statistically similar to that of Anderson et al. (2021).

3.2.5. Effects of Magnesium Concentration

Magnesium concentration in dolomite samples used for this study (where measured) ranges from 42% to 52%, with most samples between 48% and 50%, where 50% is stoichiometric dolomite. The two samples with the lowest magnesium concentration (100-A3 and Leeds 20) show very small residuals from the Anderson et al. (2021) calibration (Figure S6 in Supporting Information S1). Samples with magnesium concentrations closer to stoichiometric dolomite show a broad range of offsets from Anderson et al. (2021). There does not appear to be a systematic trend between magnesium concentration and Δ_{47} (see Figure S6 in Supporting Information S1). This is corroborated by comparing calibration regressions for samples above and below an arbitrary magnesium concentration cutoff of 49%; calibrations are statistically identical between the two subsets. Ultimately, we see no evidence that magnesium concentration affects Δ_{47} in this data set, in agreement with the conclusions of Bonifacie et al. (2017).

3.2.6. Effects of Dolomite Cation Ordering

The degree of dolomite cation ordering has been hypothesized to influence oxygen and clumped isotope compositions (Bonifacie et al., 2017; Müller et al., 2019; Winkelstern et al., 2016). All three studies concluded that dolomite ordering did not affect Δ_{47}, but each study has a narrow range of ordering ratios that cannot be compared to each other without I-CDES standards. By comparing samples from two of these data sets measured on an identical analytical setup, we can directly compare the ordering ratio. A clear relationship between ordering ratio

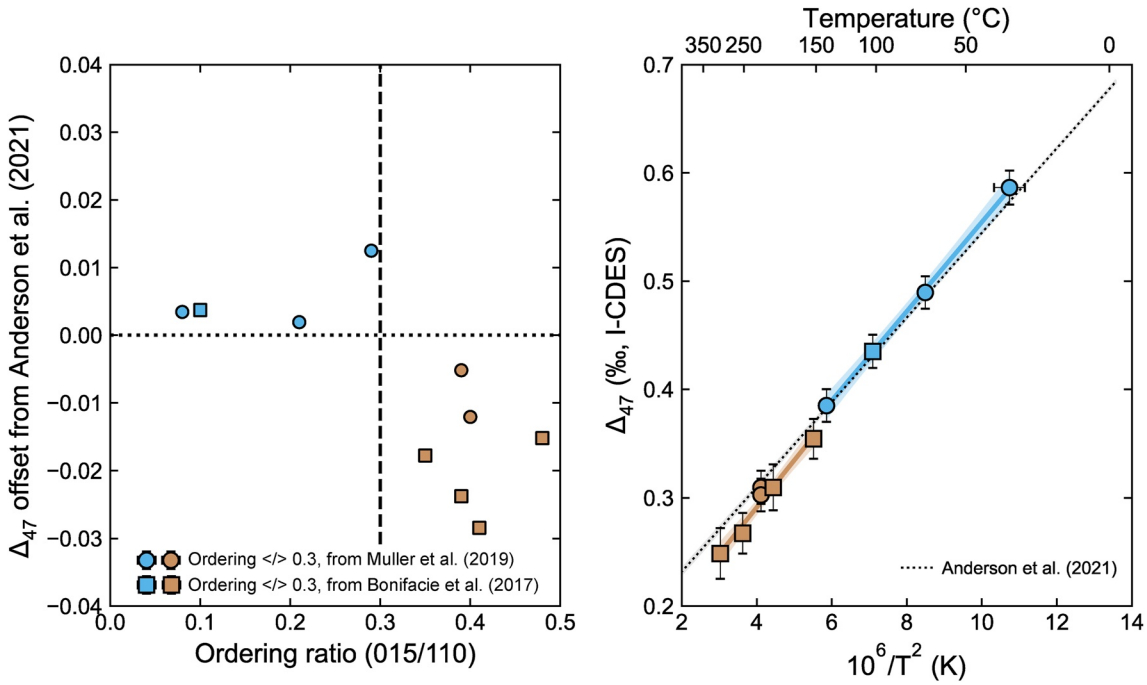

Figure 6. (a) Ordering of dolomite as measured by the ratio of (015) to (110) XRD spectra peaks compared with offset from Anderson et al. (2021) calibration; "well-ordered" samples, here arbitrarily defined as ordering ratio of 0.3, tend to fall further from the Anderson et al. (2021) calibration. Squares show Bonifacie et al. (2017) samples, circles show Müller et al. (2019) samples. (b) Comparisons of calibrations only considering poorly or well-ordered dolomites. Poorly ordered dolomites define a statistically indistinguishable calibration to that of Anderson et al. (2021); well-ordered samples do not.

and Δ_{47} would suggest the need for a mineral-specific Δ_{47}-T relationship, as "more dolomitic" (i.e., more highly ordered) samples would be expected to have "more dolomitic" Δ_{47} values.

Samples were divided into "poorly ordered" and "well-ordered" subsets at an arbitrary (015/110) ordering peak reflection ratio of 0.3 (Figure 6a). It is apparent that "poorly ordered" samples are close to or slightly below the expected values from the calibration of Anderson et al. (2021), whereas "well-ordered" samples are above (Figure 6a), potentially indicative of some true effect. Beyond this bifurcation, there is no trend to the Δ_{47}-ordering ratio relationship (Figure 6b). ANCOVA suggests a similar relationship between well- and poorly ordered dolomites in this data set, but suggests that poorly ordered samples define regression that is statistically similar to Anderson et al. (2021); well-ordered samples reject similarity with Anderson et al. (2021).

These observations have conflicting interpretations; the better agreement of poorly ordered dolomites with the calcite-based calibration of Anderson et al. (2021) suggests a relationship between ordering ratio and Δ_{47}, but the lack of a consistent trend in these data weakens this interpretation. Importantly, our comparison of well and poorly ordered dolomites in this study has key limitations. The two populations do not overlap in formation temperature, disallowing comparison over the same temperature range (Figure 6b). Furthermore, not all samples have XRD data, limiting the sample sizes for each population to $n = 4$ and $n = 6$, respectively. Importantly, many of the well-ordered samples measured here also have extremely depleted bulk isotopic compositions that are poorly constrained by the I-CDES reference frame, as discussed above. The two well-ordered samples with δ^{47} values inside the reference frame (Figure 6) and precipitated from an amorphous gel phase (see section below) show close agreement with the calibration of Anderson et al. (2021), possibly indicating that dolomite ordering is not significant. Ultimately, the data presented here are insufficient to determine if dolomite ordering is a possible cause of differences in calibration regressions. Future dolomite clumped isotope calibrations should strive to create samples formed at similar temperatures (ideally at several of a broad range of temperatures) that vary in dolomite cation ordering to explicitly test this potential effect.

3.2.7. Effect of Precipitation Kinetics

Samples in this study were precipitated using four distinct methods. While it is unclear how kinetic effects specific to each process could influence sample Δ_{47}, samples from each method tend to have their own consistent

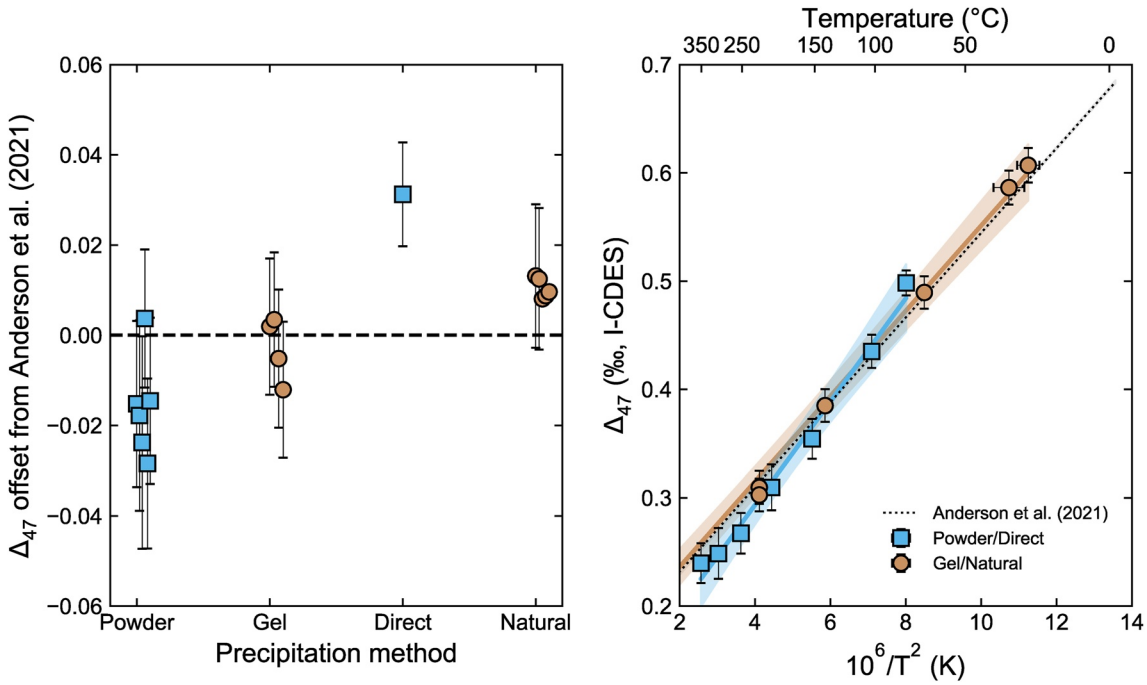

Figure 7. (a) Comparison of offsets from Anderson et al. (2021) predicted values and values measured in this study using precipitation method. Samples precipitated from amorphous gels and natural precipitates (brown circles) have lower residuals than dolomitized powders and direct precipitates (blue squares). (b) Regression of samples precipitated from amorphous gels and natural precipitates compared to that of direct precipitates and dolomitized powders. The former agrees more closely with Anderson et al. (2021).

offset from the calcite calibration (see Figure 7). Thus, we must consider that the precipitation method conferred a kinetic isotope effect, even if the mechanism is unknown.

Modern natural samples from Qatar and Brazil were precipitated in hypersaline seawater. Samples created by Horita (2014) and measured by Bonifacie et al. (2017) were formed by reacting powdered $CaCO_3$ with Ca-Mg-(Na)-Cl solutions (similar to the method used in Winkelstern et al., 2016) except for 80-1, which was directly precipitated from a solution of $MgSO_4$, $Ca(NO_3)_2{\cdot}4H_2O$, and Na_2CO_3. Samples from Müller et al. (2019) were precipitated from room temperature mixture of equimolar aqueous solutions of Na_2CO_3, $CaCl_2$, and $MgCl_2$ (Rodriguez-Blanco et al., 2015) that initially formed an amorphous gel phase.

Dolomitized powder samples ($n = 6$) and direct laboratory precipitates ($n = 1$) have offsets of 21 and 31 ppm from Anderson et al. (2021) values, while dolomitized amorphous gels ($n = 4$) and natural precipitates ($n = 5$) have offsets of 6 and 10 ppm, respectively. Excluding dolomitized powders and direct precipitates causes statistical convergence of the calibration regression from this study with that of Anderson et al. (2021). Without a specific mechanism to explain why dolomitization of a solid versus precipitation from an amorphous gel could confer a potential isotope effect, we cannot conclude that precipitation method influences Δ_{47} of these carbonates. We speculate that the dolomitization of powdered $CaCO_3$ samples more closely represents diagenetic dolomite, whereas precipitation from an amorphous precursor phase approximates primary precipitation of dolomite from seawater (Rodriguez-Blanco et al., 2015).

3.2.8. Consolidating and Comparing Carbonate-Standardized Dolomite Calibrations

Because Müller et al. (2019) used InterCarb standards to establish a reference frame, those data can be recalculated with the I-CDES values, compared within the same framework, and consolidated with the data presented in this study to create a stronger calibration. ANCOVA suggests that the calibration equations defined by combining the data from this study and Müller et al. (2019) statistically agree with Anderson et al. (2021) in both slope and intercept.

We note that a subset of samples in Figures 5–7 (squares in each figure) represents all samples with extremely depleted bulk isotopic compositions, most samples with stronger ordering peaks, and all dolomitized powder

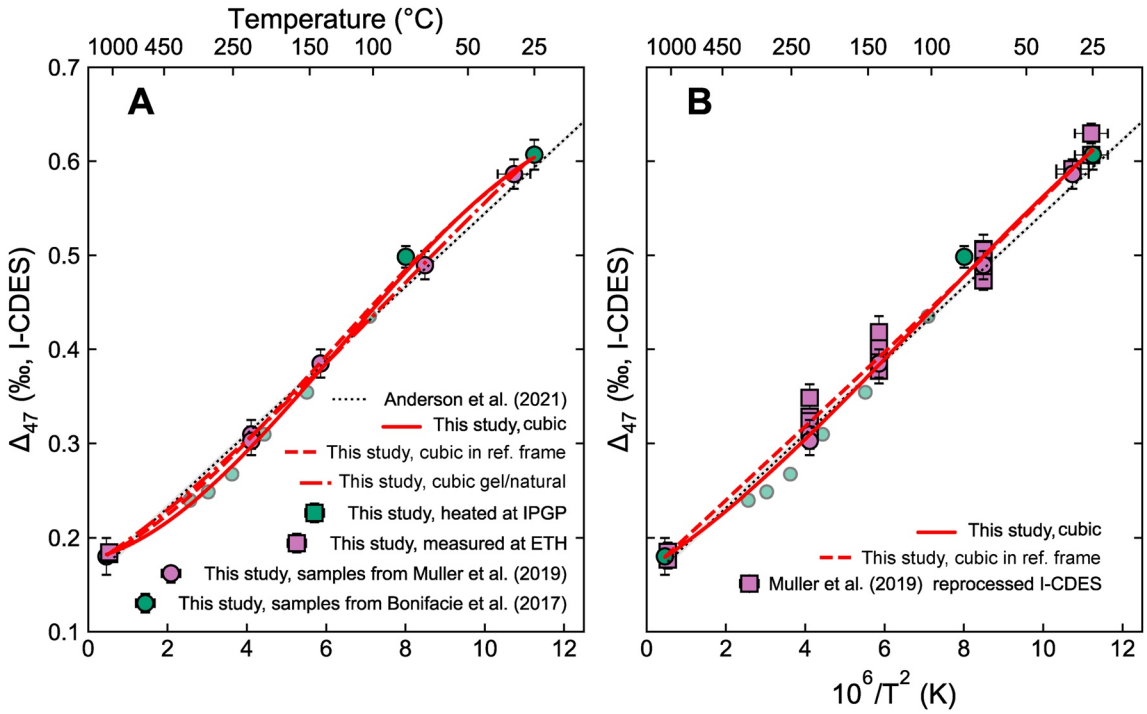

Figure 8. (a) Comparison of third-order polynomial regressions with all data with $\delta^{47} > -30$ (dashed) and all natural or amorphous gel precipitates (dash-dot); the latter is within 1 SD of the third-order polynomial regression of Anderson et al. (2021). Third-order polynomials show high sensitivity to the removal of individual samples. (b) Same as plot from A but including reprocessed data from Müller et al. (2019).

samples. It is possible that any of these specific characteristics explain their consistent offset to Anderson et al. (2021) and that such samples should be treated cautiously when attempting to calibrate dolomite writ large. Given that they are always most of the samples excluded in each test above, that higher replication of these samples increases their relative weight in calibration equations, and that this group of samples are the sole representatives between 220 and 1,100°C, we explore removing this entire population of samples here.

When only samples from this study that are well constrained by the I-CDES reference frame and are produced from dolomitized powder are considered (circles in Figures 5–7), ANCOVA suggests agreement between this study and Anderson et al. (2021) for slope but not intercept, although the slopes and intercepts are within 1 SD of each other (Figure 1, Table 3). Using this subset of the data, the offset in calculated temperature between this study and Anderson et al. (2021) is slightly worse: 3–4°C at Earth-surface temperatures (Figure 2). Composite regression of reprocessed Müller et al. (2019) data and samples from this study without the above-mentioned characteristics shows agreement from ANCOVA with the calibration of Anderson et al. (2021) in the slope but not in intercept. These calibrations agree within 1SD of the linear regression intercept but not slope. If we also exclude sample 80-1, which did not quantitatively dissolve in phosphoric acid and is the only laboratory sample to be formed from the direct precipitation of dolomite (Figure 7), ANCOVA suggests agreement between this study and Anderson et al. (2021; Table 3).

For third order regressions, excluding poorly constrained/dolomitized powder samples from the regression leads to agreement with third-order regression from Anderson et al. (2021) within 1 SD for all four regression coefficients. However, when reprocessed data from Müller et al. (2019) are added, only one coefficient agrees; however, if sample 80-1 is removed, all coefficients agree (Figure 8, Table S4). These results demonstrate that third-order regressions are highly sensitive to individual samples when data density is low. For this reason, we caution against using non-linear regressions for dolomite calibrations until (a) data density increases or (b) potential causes for deviation from linear relationships are better understood.

These results do not provide unequivocal support for the interchangeability of dolomite and calcite clumped isotope calibrations but several lines of evidence point to strong agreement. Most (dis)agreement depends on the choice of samples, regression method, and how equations are compared. However, the (a) statistical

indistinguishability of calcite versus dolomite calibrations for linear regressions, (b) statistical indistinguishability of third-order calcite and dolomite regressions when a population of samples with extremely depleted bulk isotopic composition were excluded, and (c) similarity between near-stochastic dolomites and calcites lead us to suggest that a dolomite-specific clumped isotope calibration is unnecessary. This conclusion aligns with the theoretical literature that shows minimal discrepancy between clumped isotope equilibrium between dolomite and calcite (Hill et al., 2020; Schauble et al., 2006). The higher uncertainty of the calibration equation from data in this study compared to for example, Anderson et al. (2021; 0.0006 versus 0.0004 on slope) provide another reason to use recent calcite-based calibrations (Anderson et al., 2021; Fiebig et al., 2021; Jautzy et al., 2021; Petersen et al., 2019) for dolomite in the absence of strong evidence for a dolomite-specific calibration.

While we suggest that dolomite-specific regression is unnecessary, more dolomite calibration data, ideally projected into the I-CDES, run alongside dolomite standards including Rodolo and SRM-88b with community consensus values (cf. Bernasconi et al., 2021) and with consistent sample characteristics is necessary to provide an unequivocal verdict on potential differences between dolomite and calcite calibrations.

3.3. Calibration of the Apatite Clumped Isotope Thermometer

3.3.1. Comparison With Previous Calcite and Apatite Calibrations

The apatite-specific calibration reported here (Figure 9) is within the error of the Anderson et al. (2021) calibration. ANCOVA analysis does not reject the null hypothesis of identical slope/intercept between the two calibrations, nor between the apatite calibration from this study and that of Löffler et al. (2019) or Griffiths et al. (2023; see Table 3). The calibration of Löffler et al. (2019; when an AFF of 0.018‰ is applied to correct values to 90°C) and Griffiths et al. (2023) are also within the error envelope of the apatite calibration presented in this study (Figure 9). Data from Löffler et al. (2019) were corrected to the $CDES_{90°C}$ using the acid fractionation factor proposed in Defliese et al. (2015), although we note that this AFF was determined for calcite, not apatite, which may introduce additional uncertainty into the comparison. While Löffler et al. (2019) did measure InterCarb standards alongside their unknowns, the overall low number of InterCarb anchors (1:2 anchor:unknown ratio) and strong bias toward ETH-3 (41 analyses vs. 8 of ETH-2 and 12 of ETH-4) do not facilitate projection into the I-CDES.

This result suggests shows strong interlaboratory agreement in measurements of unique apatite samples, regardless of if InterCarb standards are used to correct data, and that apatite calibrations give statistically indistinguishable results from calcite calibrations, in agreement with the past empirical calibrations as well as theoretical calculations (Eagle et al., 2010; Griffiths et al., 2023; Löffler et al., 2019). Furthermore, while not a direct test of sample pretreatment protocols, the strong agreement of untreated apatites used in this study and Löffler et al. (2019) with hydrogen peroxide and buffered acetic treatment used in Griffiths et al. (2023) points to insensitivity of apatites to pretreatment method. We also show that apatite measurements at an acid reaction temperature of 70°C with relatively small sample sizes (~400 μg carbonate; 5–20 mg apatite) are comparable to hotter and larger digestions.

Because the apatite calibration presented here is defined only by five unique samples that span a relatively narrow temperature range, we strongly recommend that the statistically equivalent and much better-defined calibrations for calcite are used (e.g., Anderson et al., 2021; Fiebig et al., 2021; Jautzy et al., 2021; Petersen et al., 2019) to calculate values for apatites formed near Earth surface temperatures (<40°C). We do not have data above 40°C, at which point the Löffler et al. (2019) calibration diverges strongly (shallower slope) from the Anderson et al. (2021) calibration, although the divergence is driven by a single synthetic sample from Löffler et al. (2019). As such, it remains unclear if high-temperature apatites show a true discrepancy from calcites, although theoretical apatite clumping equilibria suggest that apatite and calcite measurements are nearly indistinguishable (Eagle et al., 2010). Analyses of exceptionally high temperature natural apatites (>40°C) and hot synthetic apatites are necessary to extend the temperature range of this empirical calibration beyond approximately 40°C. However, our results suggest that established calcite clumped isotope calibration equations can be confidently used for calculating apatite temperatures in the temperature range of complex life.

3.3.2. Considerations for Apatite as a Paleothermometer

The high crystallinity and low crystal defects of apatite confer a resistance to post-depositional isotopic alteration that is especially useful for deep-time applications of the clumped isotope paleothermometer. However, bioapatite presents some unique challenges and opportunities that must be considered before it is used widely.

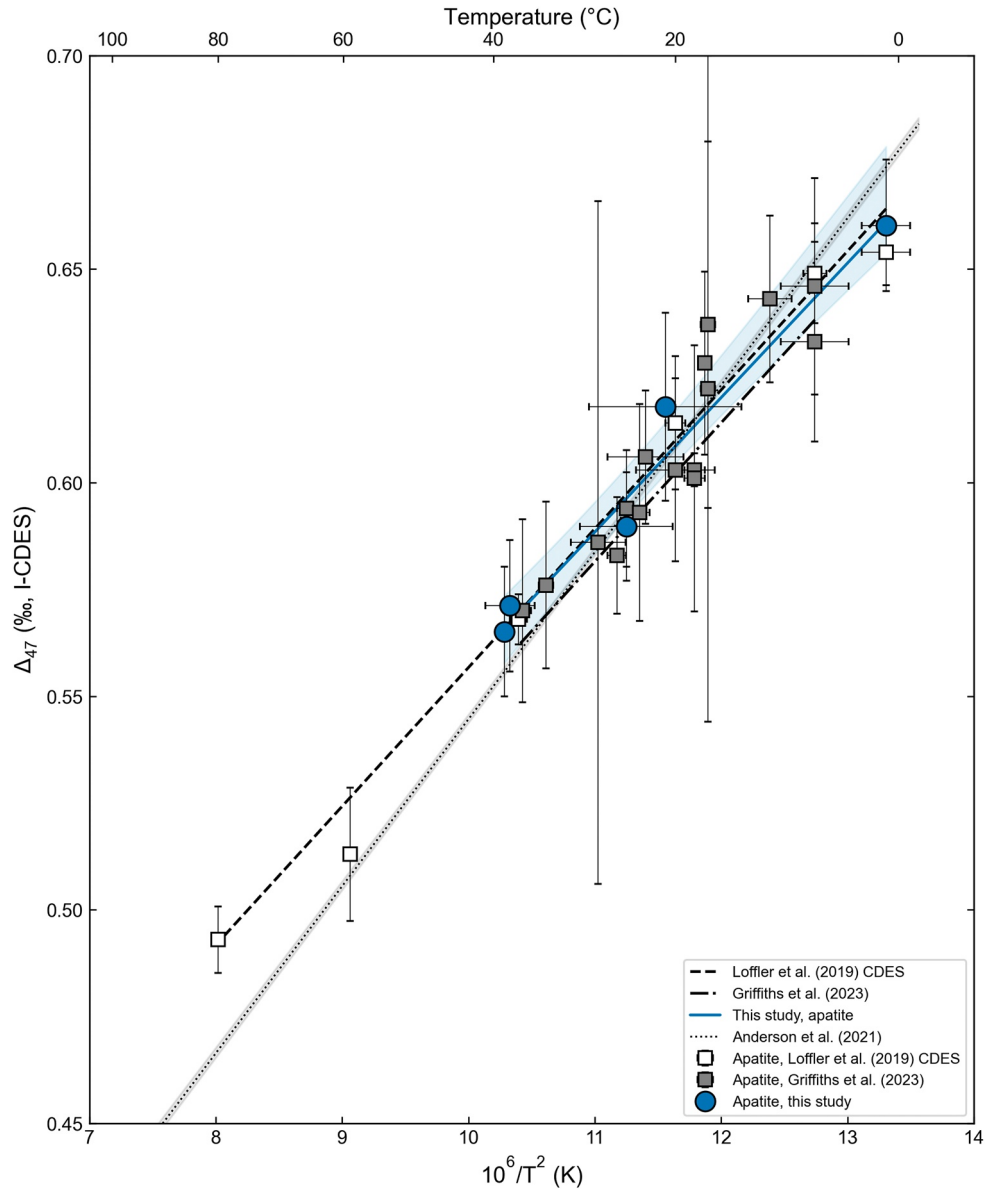

Figure 9. Linear $1/T^2$-Δ_{47} regression and 95% CI for apatite samples measured in this study (blue circles) and that from Löffler et al. (2019; open squares) and Griffiths et al. (2023; gray squares). The apatite regression from this study agrees with the regressions of both Anderson et al. (2021), Griffiths et al. (2023), and Löffler et al. (2019).

Some modern bioapatite samples have high organic matter preservation (e.g., inarticulate brachiopods) of up to ~50% which produces anomalous Δ_{47} values (Bergmann et al., 2018). A variety of cleaning procedures have been used to eliminate organic material, including various concentrations of bleach and hydrogen peroxide (Crowley & Wheatley, 2014; Eagle et al., 2010; Griffiths et al., 2023; Key et al., 2020; Löffler et al., 2019; Pellegrini & Snoeck, 2016; Wacker et al., 2016). Some of these studies have shown disagreement in sample Δ_{47} and/or $\delta^{18}O$ between treated and untreated samples, but excellent agreement between the untreated apatites of this study and Löffler et al., 2019 with the pretreated apatites of Griffiths et al. (2023) supports our decision to avoid pretreatment. We note that Eagle et al. (2010) found no effect of pre-treatment on clumped isotope analyses of enamel but found an effect on analyses of dentine, suggesting that organic-rich apatites could be significantly affected by sample pre-treatment. Because we measured organic-poor enamel in this study, we follow the recommendations of Eagle et al. (2010), Key et al. (2020), Löffler et al. (2019), and Wacker et al. (2016) and opt not to pre-treat apatite samples.

Another source of uncertainty in paleothermometry of bioapatites involves animal behavior and seasonal cycles. Migration, whether seasonal (e.g., between feeding and mating locations) or even daily (i.e., diel vertical migration), can dramatically change the water temperature that marine organisms experience and that is ultimately recorded by the isotopic composition of their tooth enamel. In reptiles, behaviors such as basking can cause body temperature to change significantly throughout any given time interval and may be dependent on a multitude of factors. Some of these confounding variables can be independently constrained and corrected for, but some cannot and several individuals from a given time interval should be measured to give a realistic approximation of average paleotemperature. Additionally, sedimentological context should be used to independently constrain growth habitat.

4. Conclusions

We present calibrations for the dolomite and apatite clumped isotope thermometers alongside a suite of non-InterCarb standards, all corrected using carbonate anchors defined by the InterCarb exercise. We find that apatites measured here define a calibration equation that is statistically indistinguishable from Anderson et al. (2021) and suggest that any I-CDES anchored calibration equation (e.g., Anderson et al., 2021; Fiebig et al., 2021; Jautzy et al., 2021) is suitable to calculate apatite formation temperatures in labs that use carbonate standardization. These calibrations, as well as that of Petersen et al. (2019), are suitable for labs that use heated and equilibrated gases.

Dolomite calibrations from data in this study as well as all samples that can be confidently projected into the I-CDES variably (dis)agree with previous calcite calibrations depending on the order of the regression, statistical comparison method, and sample selection. Excellent agreement of heated dolomites with heated calcites suggests that there is no resolvable difference in absolute acid fractionation factor between dolomite and calcite. Further work should include samples that span a range of dolomite cation ordering and have formation temperatures that fill gaps in current I-CDES calibrations (40–100°C; 350–1,100°C).

While we cannot unequivocally show that calcite and dolomite $T\Delta_{47}$ can be described using the same calibration, but we recommend that, as with apatite, the clumped isotope community use any of the recent I-CDES calibrations to calculate dolomite formation temperature. We urge the community to select, measure, and establish accepted values for dolomite anchors that span a wide range of Δ_{47} and δ^{47} and include them regularly when measuring dolomite unknowns to facilitate laboratory intercomparison.

Data Availability Statement

All sample and analysis-level clumped isotope data are available in the EarthChem database at Anderson et al. (2024).

Acknowledgments
We thank the members of the Bergmann Lab for their help in instrument maintenance and contributions to discussions of this manuscript. This work was supported by the J.H. and E.V. Wade Fund, the mTerra Catalyst Grant, the Packard Foundation Fellowship, NASA Exobiology Grant 80NSSC19K0464, and NSF Grant 2221963. We thank the two anonymous reviewers for a detailed and thoughtful review.

References

Anderson, N. T., Bonifacie, M., Jost, A. B., Siebert, J., Bontognali, T., Horita, J., et al. (2024). Clumped isotope calibration data for dolomite and apatite; non-InterCarb carbonate standard data [Dataset]. Version 1.0. Interdisciplinary Earth Data Alliance (IEDA). https://doi.org/10.60520/IEDA/113081

Anderson, N. T., Kelson, J. R., Kele, S., Daëron, M., Bonifacie, M., Horita, J., et al. (2021). A unified clumped isotope thermometer calibration (0.5–1,100°C) using carbonate-based standardization. *Geophysical Research Letters*, *48*(7), 1–11. https://doi.org/10.1029/2020gl092069

Barney, B. B., & Grossman, E. L. (2022). Reassessment of ocean paleotemperatures during the Late Ordovician. *Geology*, *50*, 1–5. https://doi.org/10.1130/G49422.1/5543257/g49422.pdf

Bergmann, K. D., Finnegan, S., Creel, R., Eiler, J. M., Hughes, N. C., Popov, L. E., & Fischer, W. W. (2018). A paired apatite and calcite clumped isotope thermometry approach to estimating Cambro-Ordovician seawater temperatures and isotopic composition. *Geochimica et Cosmochimica Acta*, *224*, 18–41. https://doi.org/10.1016/j.gca.2017.11.015

Bernasconi, S. M., Daëron, M., Bergmann, K. D., Bonifacie, M., Meckler, A. N., Affek, H. P., et al. (2021). InterCarb: A community effort to improve inter-laboratory standardization of the carbonate clumped isotope thermometer using carbonate standards. *Geochemistry, Geophysics, Geosystems*, *22*(5), 1–25. https://doi.org/10.1029/2020gc009588

Bernasconi, S. M., Müller, I. A., Bergmann, K. D., Breitenbach, S. F. M., Fernandez, A., Hodell, D. A., et al. (2018). Reducing uncertainties in carbonate clumped isotope analysis through consistent carbonate-based standardization. *Geochemistry, Geophysics, Geosystems*, *19*(9), 2895–2914. https://doi.org/10.1029/2017GC007385

Bonifacie, M., Anderson, N. T., Bergmann, K. D., Katz, A., Calmels, D., Siebert, J., et al. (2023). Do we need to have mineral-specific Δ_{47}: Calibrations and/or acid fractionation factors and/or community standards? In *Goldschmidt conference*.

Bonifacie, M., Calmels, D., Eiler, J. M., Horita, J., Chaduteau, C., Vasconcelos, C., et al. (2017). Calibration of the dolomite clumped isotope thermometer from 25 to 350°C, and implications for a universal calibration for all (Ca, Mg, Fe)CO_3 carbonates. *Geochimica et Cosmochimica Acta*, *200*, 255–279. https://doi.org/10.1016/j.gca.2016.11.028

Brauchli, M., McKenzie, J. A., Strohmenger, C. J., Sadooni, F., Vasconcelos, C., & Bontognali, T. R. R. (2016). The importance of microbial mats for dolomite formation in the Dohat Faishakh sabkha, Qatar. *Carbonates and Evaporites*, *31*(3), 339–345. https://doi.org/10.1007/s13146-015-0275-0

Brigaud, B., Bonifacie, M., Pagel, M., Blaise, T., Calmels, D., Haurine, F., et al. (2020). Past hot fluid flows in limestones detected by Δ_{47}–(U-Pb) and not recorded by other geothermometers. *Geology*, *48*(9), 851–856. https://doi.org/10.1130/g47358.1

Butler, G. P. (1969). Modern evaporite deposition and geochemistry of coexisting brines, the Sabkha, Trucial Coast, Arabian Gulf. *Journal of Sedimentary Petrology*, *39*, 70–89. https://doi.org/10.1306/74d71be5-2b21-11d7-8648000102c1865d

Came, R. E., Azmy, K., Tripati, A., & Olanipekun, B. J. (2017). Comparison of clumped isotope signatures of dolomite cements to fluid inclusion thermometry in the temperature range of 73–176°C. *Geochimica et Cosmochimica Acta*, *199*, 31–47. https://doi.org/10.1016/j.gca.2016.10.028

Clarke, A., Rothery, P., & Isaac, N. J. B. (2010). Scaling of basal metabolic rate with body mass and temperature in mammals. *Journal of Animal Ecology*, *79*(3), 610–619. https://doi.org/10.1111/j.1365-2656.2010.01672.x

Crowley, B. E., & Wheatley, P. V. (2014). To bleach or not to bleach? Comparing treatment methods for isolating biogenic carbonate. *Chemical Geology*, *381*, 234–242. https://doi.org/10.1016/j.chemgeo.2014.05.006

Daëron, M. (2021). Full propagation of analytical uncertainties in Δ_{47} measurements. *Geochemistry, Geophysics, Geosystems*, *22*(5), e2020GC009592. https://doi.org/10.1029/2020gc009592

Defliese, W. F., Hren, M. T., & Lohmann, K. C. (2015). Compositional and temperature effects of phosphoric acid fractionation on δ^{47} analysis and implications for discrepant calibrations. *Chemical Geology*, *396*, 51–60. https://doi.org/10.1016/j.chemgeo.2014.12.018

de Winter, N. J., Witbaard, R., Kocken, I. J., Müller, I. A., Guo, J., Goudsmit, B., & Ziegler, M. (2022). Temperature dependence of clumped isotopes (Δ_{47}) in aragonite. *Geophysical Research Letters*, *49*(20), e2022GL099479. https://doi.org/10.1029/2022GL099479

Eagle, R. A., Schauble, E. A., Tripati, A. K., Tutken, T., Hulbert, R. C., & Eiler, J. M. (2010). Body temperatures of modern and extinct vertebrates from ^{13}C-^{18}O bond abundances in bioapatite. *Proceedings of the National Academy of Sciences*, *107*(23), 10377–10382. https://doi.org/10.1073/pnas.0911115107

Eiler, J. M. (2007). "Clumped-isotope" geochemistry-The study of naturally-occurring, multiply-substituted isotopologues. *Earth and Planetary Science Letters*, *262*(3–4), 309–327. https://doi.org/10.1016/j.epsl.2007.08.020

Fiebig, J., Daëron, M., Bernecker, M., Guo, W., Schneider, G., Boch, R., et al. (2021). Calibration of the dual clumped isotope thermometer for carbonates. *Geochimica et Cosmochimica Acta*, *312*, 235–256. https://doi.org/10.1016/j.gca.2021.07.012

García Del Cura, M. A., Calvo, J. P., Ordóñez, S., Jones, B. F., & Cañaveras, J. C. (2001). Petrographic and geochemical evidence for the formation of primary, bacterially induced lacustrine dolomite: La Roda 'white earth' (Pliocene, central Spain). *Sedimentology*, *48*(4), 897–915. https://doi.org/10.1046/j.1365-3091.2001.00388.x

Gasparrini, M., Morad, D., Mangenot, X., Bonifacie, M., Morad, S., Nader, F. H., & Gerdes, A. (2023). Dolomite recrystallization revealed by Δ_{47}/U-Pb thermochronometry in the Upper Jurassic Arab Formation, United Arab Emirates. *Geology*, *51*, 471–475. https://doi.org/10.1130/G50960.1

Ghosh, P., Adkins, J., Affek, H., Balta, B., Guo, W., Schauble, E. A., et al. (2006). ^{13}C-^{18}O bonds in carbonate minerals: A new kind of paleothermometer. *Geochimica et Cosmochimica Acta*, *70*(6), 1439–1456. https://doi.org/10.1016/j.gca.2005.11.014

Goldberg, S. L., Present, T. M., Finnegan, S., & Bergmann, K. D. (2021). A high-resolution record of early Paleozoic climate. *Proceedings of the National Academy of Sciences of the United States of America*, *118*(6), e2013083118. https://doi.org/10.1073/pnas.2013083118

Griffiths, M. L., Eagle, R. A., Kim, S. L., Flores, R. J., Becker, M. A., Maisch, H. M., et al. (2023). Endothermic physiology of extinct megatooth sharks. *Proceedings of the National Academy of Sciences*, *120*(27), e2218153120. https://doi.org/10.1073/pnas.2218153120

Guo, W., Mosenfelder, J. L., Goddard, W. A., & Eiler, J. M. (2009). Isotopic fractionations associated with phosphoric acid digestion of carbonate minerals: Insights from first-principles theoretical modeling and clumped isotope measurements. *Geochimica et Cosmochimica Acta*, *73*(24), 7203–7225. https://doi.org/10.1016/j.gca.2009.05.071

Hawley, A. W., & Peden, D. G. (1982). Effects of ration, season and animal handling on composition of bison and cattle blood. *Journal of Wildlife Diseases*, *18*(3), 321–338. https://doi.org/10.7589/0090-3558-18.3.321

Hemingway, J. D., & Henkes, G. A. (2020). A distributed activation energy model for clumped isotope bond reordering in carbonates. *Earth and Planetary Science Letters*, *566*, 116962. https://doi.org/10.1016/j.epsl.2021.116962

Henkes, G. A., Passey, B. H., Grossman, E. L., Shenton, B. J., Yancey, T. E., & Pérez-Huerta, A. (2018). Temperature evolution and the oxygen isotope composition of Phanerozoic oceans from carbonate clumped isotope thermometry. *Earth and Planetary Science Letters*, *490*, 40–50. https://doi.org/10.1016/j.epsl.2018.02.001

Hill, P. S., Schauble, E. A., & Tripati, A. (2020). Theoretical constraints on the effects of added cations on clumped, oxygen, and carbon isotope signatures of dissolved inorganic carbon species and minerals. *Geochimica et Cosmochimica Acta*, *269*, 496–539. https://doi.org/10.1016/j.gca.2019.10.016

Holme, E. A., Henkes, G. A., Tosca, N. J., Rasbury, T. E., Young, J. M., Schaub, D. R., et al. (2022). Experimental constraints on siderite clumped isotope thermometry. *Geochimica et Cosmochimica Acta*, *343*, 323–340. https://doi.org/10.1016/j.gca.2022.12.012

Horita, J. (2014). Oxygen and carbon isotope fractionation in the system dolomite-water-CO_2 to elevated temperatures. *Geochimica et Cosmochimica Acta*, *129*, 111–124. https://doi.org/10.1016/j.gca.2013.12.027

Huntington, K. W., Eiler, J. M., Affek, H. P., Guo, W., Bonifacie, M., Yeung, L. Y., et al. (2009). Methods and limitations of "clumped" CO_2 isotope (Δ_{47}) analysis by gas-source isotope ratiomass spectrometry. *Journal of Mass Spectrometry*, *44*(9), 1318–1329. https://doi.org/10.1002/jms.1614

Illing, L. V., Wells, A. J., & Taylor, J. C. M. (1965). Penecontemporary dolomite in the Persian Gulf. In L. C. Pray & R. C. Murray (Eds.), *Dolomitization and limestone diagenesis* (pp. 89–111). SEPM Special Publication.

Jautzy, J. J., Savard, M. M., Dhillon, R. S., Bernasconi, S. M., Lavoie, D., & Smirnoff, A. (2021). Clumped isotope temperature calibration for calcite: Bridging theory and experimentation. *Geochemical Perspective Letters*, *1*(2009), 36–41. https://doi.org/10.7185/geochemlet.2021

Kele, S., Breitenbach, S. F. M., Capezzuoli, E., Meckler, A. N., Ziegler, M., Millan, I. M., et al. (2015). Temperature dependence of oxygen- and clumped isotope fractionation in carbonates: A study of travertines and tufas in the 6-95°C temperature range. *Geochimica et Cosmochimica Acta*, *168*, 172–192. https://doi.org/10.1016/j.gca.2015.06.032

Kelson, J. R., Huntington, K. W., Schauer, A. J., Saenger, C., & Lechler, A. R. (2017). Toward a universal carbonate clumped isotope calibration: Diverse synthesis and preparatory methods suggest a single temperature relationship. *Geochimica et Cosmochimica Acta*, *197*, 104–131. https://doi.org/10.1016/j.gca.2016.10.010

Kelson, J. R., Petersen, S. V., Niemi, N., Passey, B. H., & Curley, A. N. (2022). Looking upstream with clumped and triple oxygen isotopes of estuarine oyster shells in the early Eocene of California. *Geology*, *50*(7), 755–759. https://doi.org/10.1130/G49634.1/5583260/g49634.pdf

Key, M. M., Smith, A. M., Phillips, N. J., & Forrester, J. S. (2020). Effect of removal of organic material on stable isotope ratios in skeletal carbonate from taxonomic groups with complex mineralogies. *Rapid Communications in Mass Spectrometry*, *34*(20), 1–19. https://doi.org/10.1002/rcm.8901

Kim, S. T., Mucci, A., & Taylor, B. E. (2007). Phosphoric acid fractionation factors for calcite and aragonite between 25 and 75°C: Revisited. *Chemical Geology*, *246*(3–4), 135–146. https://doi.org/10.1016/j.chemgeo.2007.08.005

Koch, P. L., Tuross, N., & Fogel, M. L. (1997). The effects of sample treatment and diagenesis on the isotopic integrity of carbonate in biogenic hydroxylapatite. *Journal of Archaeological Science*, *24*(5), 417–429. https://doi.org/10.1006/jasc.1996.0126

Lang, J. W. (1979). Thermophilic response of the American alligator and the American crocodile to feeding. *American Society of Ichthyologists and Herpetologists*, *1979*(1), 48–59. https://doi.org/10.2307/1443728

LeGeros, R. Z. (1981). Apatites in biological systems. *Progress in Crystal Growth and Characterization*, *4*(1–2), 1–45. https://doi.org/10.1016/0146-3535(81)90046-0

Lloyd, M. K., Ryb, U., & Eiler, J. M. (2018). Experimental calibration of clumped isotope reordering in dolomite. *Geochimica et Cosmochimica Acta*, *242*(August), 1–20. https://doi.org/10.1016/j.gca.2018.08.036

Löffler, N., Fiebig, J., Mulch, A., Tütken, T., Schmidt, B. C., Bajnai, D., et al. (2019). Refining the temperature dependence of the oxygen and clumped isotopic compositions of structurally bound carbonate in apatite. *Geochimica et Cosmochimica Acta*, *253*, 19–38. https://doi.org/10.1016/j.gca.2019.03.002

Lu, C., Murray, S., Koeshidayatullah, A., & Swart, P. K. (2022). Clumped isotope acid fractionation factors for dolomite and calcite revisited: Should we care? *Chemical Geology*, *588*, 120637. https://doi.org/10.1016/j.chemgeo.2021.120637

Lucarelli, J. K., Carroll, H. M., Ulrich, R. N., Elliott, B. M., Coplen, T. B., Eagle, R. A., & Tripati, A. (2023). Equilibrated gas and carbonate standard-derived dual (Δ_{47} and Δ_{48}) clumped isotope values. *Geochemistry, Geophysics, Geosystems*, *24*(2), e2022GC010458. https://doi.org/10.1029/2022GC010458

Mackey, T. J., Jost, A. B., Creveling, J. R., & Bergmann, K. D. (2020). A decrease to low carbonate clumped isotope temperatures in Cryogenian strata. *AGU Advances*, *1*(3), e2019av000159. https://doi.org/10.1029/2019av000159

Mangenot, X., Gasparrini, M., Rouchon, V., & Bonifacie, M. (2018). Basin-scale thermal and fluid flow histories revealed by carbonate clumped isotopes (Δ_{47}) – Middle Jurassic carbonates of the Paris Basin depocentre. *Sedimentology*, *65*(1), 123–150. https://doi.org/10.1111/sed.12427

Meckler, A. N., Sexton, P. F., Piasecki, A. M., Leutert, T. J., Marquardt, J., Ziegler, M., et al. (2022). Cenozoic evolution of deep ocean temperature from clumped isotope thermometry. *Science*, *90*(6601), 86–90. https://doi.org/10.1126/science.abk0604

Meinicke, N., Ho, S. L., Hannisdal, B., Nürnberg, D., Tripati, A., Schiebel, R., & Meckler, A. N. (2020). A robust calibration of the clumped isotopes to temperature relationship for foraminifers. *Geochimica et Cosmochimica Acta*, *270*, 160–183. https://doi.org/10.1016/j.gca.2019.11.022

Modestou, S. E., Leutert, T. J., Fernandez, A., Lear, C. H., & Meckler, A. N. (2020). Warm middle Miocene Indian Ocean bottom water temperatures: Comparison of clumped isotope and Mg/Ca-Based estimates. *Paleoceanography and Paleoclimatology*, *35*(11), e2020PA003927. https://doi.org/10.1029/2020PA003927

Müller, I. A., Rodriguez-Blanco, J. D., Storck, J.-C., Santilli, G., Bontognali, T. R. R., Vasconcelos, C., et al. (2019). Calibration of the oxygen and clumped isotope thermometers for (proto-) dolomite based on synthetic and natural carbonates. *Chemical Geology*, *525*, 1–17. https://doi.org/10.1016/j.chemgeo.2019.07.014

Müller, I. A., Violay, M. E. S., Storck, J. C., Fernandez, A., van Dijk, J., Madonna, C., & Bernasconi, S. M. (2017). Clumped isotope fractionation during phosphoric acid digestion of carbonates at 70°C. *Chemical Geology*, *449*, 1–14. https://doi.org/10.1016/j.chemgeo.2016.11.030

Murray, S. T., Arienzo, M. M., & Swart, P. K. (2016). Determining the Δ_{47} acid fractionation in dolomites. *Geochimica et Cosmochimica Acta*, *174*, 42–53. https://doi.org/10.1016/j.gca.2015.10.029

Pellegrini, M., & Snoeck, C. (2016). Comparing bioapatite carbonate pre-treatments for isotopic measurements: Part 2 - Impact on carbon and oxygen isotope compositions. *Chemical Geology*, *420*, 88–96. https://doi.org/10.1016/j.chemgeo.2015.10.038

Peral, M., Daëron, M., Blamart, D., Bassinot, F., Dewilde, F., Smialkowski, N., et al. (2018). Updated calibration of the clumped isotope thermometer in planktonic and benthic foraminifera. *Geochimica et Cosmochimica Acta*, *239*, 1–16. https://doi.org/10.1016/j.gca.2018.07.016

Petersen, S. V., Defliese, W. F., Saenger, C., Daëron, M., Huntington, K. W., John, C. M., et al. (2019). Effects of improved ^{17}O correction on interlaboratory agreement in clumped isotope calibrations, estimates of mineral-specific offsets, and temperature dependence of acid digestion fractionation. *Geochemistry, Geophysics, Geosystems*, *20*(7), 3495–3519. https://doi.org/10.1029/2018gc008127

Rodriguez-Blanco, J. D., Shaw, S., & Benning, L. G. (2015). A route for the direct crystallization of dolomite. *American Mineralogist*, *100*(5–6), 1172–1181. https://doi.org/10.2138/am-2015-4963

Rosenbaum, J., & Sheppard, S. M. F. (1986). An isotopic study of siderites, dolomites and ankerites at high temperatures. *Geochimica et Cosmochimica Acta*, *50*(6), 1147–1150. https://doi.org/10.1016/0016-7037(86)90396-0

Ross, S. M. (2003). Peirce's criterion for the elimination of suspect experimental data. *Journal of Engineering Technology*, *20*, 1–12.

Schauble, E. A., Ghosh, P., & Eiler, J. M. (2006). Preferential formation of ^{13}C – ^{18}O bonds in carbonate minerals, estimated using first-principles lattice dynamics. *Geochimica et Cosmochimica Acta*, *70*(10), 2510–2529. https://doi.org/10.1016/j.gca.2006.02.011

Shenton, B. J., Grossman, E. L., Passey, B. H., Henkes, G. A., Becker, T. P., Laya, J. C., et al. (2015). Clumped isotope thermometry in deeply buried sedimentary carbonates: The effects of bond reordering and recrystallization. *Bulletin of the Geological Society of America*, *127*(7–8), 1036–1051. https://doi.org/10.1130/B31169.1

Swart, P. K., Murray, S. T., Staudigel, P. T., & Hodell, D. A. (2019). Oxygen isotopic exchange between CO_2 and phosphoric acid: Implications for the measurement of clumped isotopes in carbonates. *Geochemistry, Geophysics, Geosystems*, *20*(7), 3730–3750. https://doi.org/10.1029/2019gc008209

Upadhyay, D., Lucarelli, J., Arnold, A., Flores, R., Bricker, H., Ulrich, R. N., et al. (2021). Carbonate clumped isotope analysis (Δ_{47}) of 21 carbonate standards determined via gas-source isotope-ratio mass spectrometry on four instrumental configurations using carbonate-based standardization and multiyear data sets. *Rapid Communications in Mass Spectrometry*, *35*(17), 1–24. https://doi.org/10.1002/rcm.9143

Wacker, U., Rutz, T., Löffler, N., Conrad, A. C., Tütken, T., Böttcher, M. E., & Fiebig, J. (2016). Clumped isotope thermometry of carbonate-bearing apatite: Revised sample pre-treatment, acid digestion, and temperature calibration. *Chemical Geology*, *443*, 97–110. https://doi.org/10.1016/j.chemgeo.2016.09.009

Wang, Z., Schauble, E. A., & Eiler, J. M. (2004). Equilibrium thermodynamics of multiply substituted isotopologues of molecular gases. *Geochimica et Cosmochimica Acta*, *68*(23), 4779–4797. https://doi.org/10.1016/j.gca.2004.05.039

Watanabe, Y. Y., Goldman, K. J., Caselle, J. E., Chapman, D. D., & Papastamatiou, Y. P. (2015). Comparative analyses of animal-tracking data reveal ecological significance of endothermy in fishes. *Proceedings of the National Academy of Sciences of the United States of America*, *112*(19), 6104–6109. https://doi.org/10.1073/pnas.1500316112

Winkelstern, I. Z., Kaczmarek, S. E., Lohmann, K. C., & Humphrey, J. D. (2016). Calibration of dolomite clumped isotope thermometry. *Chemical Geology*, *443*, 32–38. https://doi.org/10.1016/j.chemgeo.2016.09.021

York, D., Evensen, N. M., López, M., & Delgado, J. D. B. (2004). Unified equations for the slope, intercept, and standard errors of the best straight line. *American Journal of Physics*, *72*(3), 367–373. https://doi.org/10.1119/1.1632486

Zaarur, S., Affek, H. P., & Brandon, M. T. (2013). A revised calibration of the clumped isotope thermometer. *Earth and Planetary Science Letters*, *382*, 47–57. https://doi.org/10.1016/j.epsl.2013.07.026